Title
Buckling of Short Beams Considering Shear Warping: Application to Fiber-Reinforced Elastomeric Isolators

Journal
Journal of Engineering Mechanics, 150(1)

ISSN
0733-9399

Authors
Montalto, Eduardo J
Konstantinidis, Dimitrios

Publication Date
2024

DOI
10.1061/jenmdt.emeng-7198

Buckling of Short Beams Considering Shear Warping with Application to Fiber-Reinforced Elastomeric Isolators

Eduardo J. Montalto[1] and Dimitrios Konstantinidis[2]

[1]Ph.D Candidate, Dept. of Civil and Environmental Engineering, Univ. of California, Berkeley, CA 94720. Email: eduardo_montalto@berkeley.edu

[2]Associate Professor, Dept. of Civil and Environmental Engineering, Univ. of California, Berkeley, CA 94720 (corresponding author). Email: konstantinidis@berkeley.edu

Abstract

This paper presents a theory for the buckling of short beams considering cross-sectional distortions due to transverse shear (i.e., shear warping), based on the consistent linearization of a geometrically nonlinear planar beam. The proposed deformation field considers the warping amplitude as an independent kinematic field, while the hyperelastic material assumes that the stresses normal and tangent to the deformed cross section are linear with respect to their work-conjugate finite strains. An approximate closed-form solution to the resulting quartic equation for the critical load is provided to facilitate practical implementation. Theoretical differences giving rise to distinct buckling theories for higher-order shear beams are discussed in terms of (1) the assumed deformation field, (2) variational consistency, and (3) material constitutive relation. The proposed formulation is applied to evaluate the stability of infinite strip unbonded fiber reinforced elastomeric isolators (FREIs) with moderate-to-high shape factor, for which shear warping is expected to have a major influence due to the flexural flexibility of the fiber reinforcement. A homogenization procedure is described to obtain effective isolator rigidities considering rubber compressibility and fiber extensibility. Next, a finite element parametric study of the buckling of unbonded infinite strip FREIs is presented and the results are used as a benchmark to evaluate the adequacy of the proposed and

existing formulations. The theory presented herein and its approximate solution exhibit the best match with the numerical results, and the latter is deemed adequate for practical application.

Author keywords: Higher-order shear beams; Shear warping; Buckling theory; Fiber reinforced elastomeric isolators (FREIs); Stability of elastomeric bearings; Seismic isolation

INTRODUCTION

Some non-slender elements, such as elastomeric seismic isolators, are susceptible to buckling under compression due to their high flexibility in shear. This can be evaluated using a beam theory for which the cross sections remain plane but not orthogonal to the deformed axis. Two main buckling theories have been developed along these lines: Engesser's (1891) and Haringx's theories (1949). The latter, which assumes the axial and shear stress resultants P and V to be oriented with respect to the deformed cross section of the beam, has shown to be more appropriate for the stability analysis of steel-reinforced elastomeric bearings where the reinforcement can be assumed to be rigid in bending (Gent 1964; Kelly and Konstantinidis 2011). Haringx's buckling load is given by:

$$P_{cr}^{H} = \frac{-P_S + \sqrt{P_S^2 + 4P_S P_E}}{2} \tag{1}$$

where $P_S = GA$ = the shear rigidity, $P_E = \pi^2 EI/h^2$ = Euler's critical load, EI = the bending rigidity, and h = height. For elastomeric isolators with flexible reinforcement such as fiber-reinforced elastomeric isolators (FREIs), the assumption that plane sections remain plane is no longer valid because of the bending flexibility of the reinforcing elements, and warping needs to be accounted for; in this paper warping refers exclusively to the cross-sectional distortions caused by transverse shear (cf. warping due to torsion often described in the context of thin-walled elements).

A plethora of planar beam theories considering shear warping, referred to as higher-order shear beams, has been proposed, and their stability under compressive loads has been explored (Wang et al. 2000; Challamel 2011; Challamel et al. 2013), albeit to a lesser extent. Within the context of elastomeric bearings, Simo (1982) studied the stability of planar elastomeric isolators accounting for the finite bending rigidity of the reinforcing plates. The cross-sectional distortion f_w was based on the solution to the 2D boundary-value problem of a sheared bearing, and the warping amplitude was taken proportional to the average shear strain $\bar{\gamma} = v' - \psi$, where v = lateral displacement of the beam and ψ = average rotation of the cross-section, leading to a closed-form solution for P_{cr}. Kelly (1994), followed by Tsai and Kelly (2005a, 2005b), studied the same problem by means of a beam theory which considers an additional generalized displacement ϕ corresponding to the warping amplitude. In this theory, hereinafter referred to as the *Kelly-Tsai theory*, the warping function f_w was defined in a way that avoids coupling of the new generalized stress resultants with the axial force P and bending moment M. A second-order approximation of the finite strain in the beam was obtained by drawing the deformed configuration of a differential element; the caveat is that finite strain measures are not unique, and a different strain would lead to a completely different theory. This theory results in a cubic equation for P_{cr}.

Both of the aforementioned theories match with that of Haringx when the reinforcement is perfectly rigid in bending, but yield vastly different results for an element with finite warping rigidity. Moreover, Simo's formulation has largely been missing from subsequent literature, while the Kelly-Tsai theory has been acknowledged (Pauletta 2019; Van Engelen 2019a) but seldom compared with experimental or numerical simulation results. The only exception is a recent study by Galano et al. (2021), which estimated the buckling of square FREIs employing equivalent two-dimensional finite element analyses, concluding that the Kelly-Tsai theory overpredicted the critical loads. However, the study implemented the equations presented by Tsai and Kelly (2005b) for a general homogeneous beam with the sole modification of using the effective compressive modulus E_c of the bearing, while the theory requires the use of effective rigidities in bending and warping (Tsai and Kelly 2005a). Other studies concerning the buckling load of unbonded FREIs (Kelly and Marsico 2010) or the influence of compressive loads on their lateral stiffness (Strauss et al. 2014; Habieb et al. 2019) have neglected warping effects and resorted to Haringx's theory.

This paper revisits the theoretical formulation of a buckling theory for short beams that accounts for shear warping, which is of particular interest for short composite elements highly flexible in shear. The theory is derived by a consistent linearization of the geometrically nonlinear planar beam. The finite deformation field assumes the amplitude of the cross-sectional warping as an independent generalized displacement ϕ. Emphasis is spent on establishing a suitable material constitutive relation for the one-dimensional theory, assuming linearity of the stresses normal and tangent to the deformed cross section with respect to their conjugate finite strains. The theory derived results in a quartic equation for the critical load P_{cr} of an element with fixed supports (i.e., no rotation or warping at the supports) but free to sway at the top support, which, upon simplification, coincides with that of the Kelly-Tsai theory. An approximate closed-form solution for P_{cr} is proposed and shown to be in excellent agreement with the exact solution. The differences giving rise to distinct buckling theories for higher-order shear beams are explored in terms of (1) the assumed deformation field, (2) the variational consistency, and (3) the material constitutive relation. The proposed theory, Simo's theory, and one of the solutions presented by Challamel (2011) (representative of alternative formulations) are discussed in this context.

The proposed and existing theories are used to analyze the stability of infinite strip unbonded FREIs with moderate-to-high shape factor and standard support conditions for seismic base isolation (i.e., neither rotation nor warping at the supports) under no initial lateral displacement. First, the effective rigidities required to compute the critical load of FREIs are introduced accounting for rubber compressibility and fiber extensibility. Then, a parametric study for the critical load of the isolators is presented using a series of two-dimensional plane strain finite element analyses, and the validity of the analytical formulations is assessed by comparing their solutions to the numerical results. The present formulation, in agreement with the Kelly-Tsai theory, presents the best match with the critical loads from the numerical simulations. The results for the infinite strip bearings provide a proof-of-concept for the analytical formulation, while its extension to evaluate the buckling of FREIs with rectangular, circular and annular cross sections will be addressed in an upcoming work by the authors. The approximate closed-form equation provides a valuable resource for the buckling checks required for the design of these devices (see Pauletta 2019). This work also serves as a cornerstone to study the stability of unbonded FREIs under lateral deformation due to seismic loading, which corresponds to their most critical design condition, in future studies.

BUCKLING THEORY

Assumed Deformation Field

The undeformed planar beam to be analyzed has a height $h \subset \mathbb{R}$ and cross section $\mathcal{A} \subset \mathbb{R}$, such that its reference configuration $\mathcal{B} \subset \mathbb{R}^2$ is given by $\mathcal{B} = \mathcal{A} \times [0, h]$. The coordinates in the reference configuration $\mathcal{B}$ are designated by $\{\mathbf{X}\} = \{X, Z\}$ and the associated orthonormal basis $\{\mathbf{E}_A\}$ with $A = 1, 2$ (see Fig. 1). It is assumed that the beam's modulus-weighted centroidal axis in the reference configuration is oriented along the Z coordinate; the material is not necessarily assumed to be homogeneous over $\mathcal{A}$. The beam's coordinates in the deformed configuration are given by $\{\mathbf{x}\} = \{x, z\}$ and the associated orthonormal basis $\{\mathbf{e}_i\}$ with $i = 1, 2$. For convenience we choose the orthonormal basis in the current configuration such that $\{\mathbf{e}_i\} = \{\mathbf{E}_A\}$. Unless otherwise stated, the components of vectors and tensors will be given with respect to the $\{\mathbf{E}_A\}$ and $\{\mathbf{e}_i\}$ bases.

The beam is subjected to a deformation $\boldsymbol{\varphi} : \mathcal{B} \to \mathbb{R}^2$ such that the position in the current configuration is given by $\mathbf{x} = \boldsymbol{\varphi}(\mathbf{X})$. The planar deformation occurring in the XZ plane assumes that plane sections do not remain plane and do not remain normal to the deformed axis of the beam. The deformation field is:

$$\boldsymbol{\varphi}(X, Z) = \boldsymbol{\varphi}_o(Z) + X\mathbf{d}_1(Z) - f_w(X)\,\phi(Z)\,\mathbf{d}_2(Z) \tag{2}$$

where the deformation of the beam's axis, $\boldsymbol{\varphi}_o(Z) = \boldsymbol{\varphi}(X = 0, Z)$, is given by:

$$\boldsymbol{\varphi}_o(Z) = v(Z)\,\mathbf{e}_1 + [Z + \Delta(Z)]\,\mathbf{e}_2 \tag{3}$$

and $\mathbf{d}_1(Z)$ and $\mathbf{d}_2(Z)$ are the unit vectors tangent and normal to the deformed cross section in the absence of warping, respectively, calculated as:

$$\mathbf{d}_1(Z) = \cos\psi(Z)\,\mathbf{e}_1 - \sin\psi(Z)\,\mathbf{e}_2 \qquad \mathbf{d}_2(Z) = \sin\psi(Z)\,\mathbf{e}_1 + \cos\psi(Z)\,\mathbf{e}_2 \tag{4}$$

The generalized displacements $\boldsymbol{\eta}(Z) = \{\Delta(Z), v(Z), \psi(Z), \phi(Z)\}$ parameterize the deformation field, where $\Delta(Z)$ and $v(Z)$ correspond to the vertical and lateral displacements of the axis, respectively, $\psi(Z)$ is the rotation of the cross section in the absence of warping, and $\phi(Z)$ is the dimensionless amplitude multiplier for the cross-sectional warping (see Fig. 1). Such a deformation field is analogous to that proposed earlier in the context of constrained director Cosserat models for nonlinear geometrically exact rods that allow for warping (e.g., Simo and Vu-Quoc 1991).

The warping function is selected such that the generalized stress resultants P, M, and Q (warping moment) are decoupled. Thus, the following conditions are enforced:

$$\int_{\mathcal{A}} f_w \sigma_{\Delta'}(X)\,dA = 0 \qquad \int_{\mathcal{A}} f_w \sigma_{\psi'}(X)\,dA = 0 \qquad \int_{\mathcal{A}} \sigma_{\phi'}(X)\,dA = 0 \qquad \int_{\mathcal{A}} X\sigma_{\phi'}(X)\,dA = 0 \tag{5}$$

where $\sigma_{\Delta'}(X)$, $\sigma_{\psi'}(X)$, $\sigma_{\phi'}(X)$ = the axial stresses caused by an axial strain Δ', a curvature ψ', and a rate of warping ϕ', respectively. For a homogeneous beam, these requirements can be restated as the following orthogonality conditions:

$$\int_{\mathcal{A}} f_w(X)\,dA = 0 \qquad \int_{\mathcal{A}} X f_w(X)\,dA = 0 \tag{6}$$

which, in the small deformation range, allow the interpretation of $\Delta(Z)$ and $v(Z)$ as the average axial and transverse displacements, respectively, and of $\psi(Z)$ as the average rotation of the cross section. For the planar element, the following function satisfying these requirements will be employed:

$$f_w(X) = \frac{5}{6}\left(\frac{X^3}{2b^2} + \omega X\right) \tag{7}$$

where b = half the cross-sectional depth. For a homogeneous beam, $\omega = -3/10$ after enforcing Eq. (6). For a non-homogeneous element, such as an elastomeric bearing, ω will need to be calculated making use of the general conditions in Eq. (5).

Kinematics

Based on the deformation field presented in Eq. (2), the components of the deformation gradient $\mathbf{F} = \partial\boldsymbol{\varphi}/\partial\mathbf{X}$ are:

$$[F_{iA}] = \begin{pmatrix} \cos(\psi) - f_w'\,\phi\sin(\psi) & v' - X\sin(\psi)\,\psi' - f_w\,\phi'\sin(\psi) - f_w\,\phi\cos(\psi)\,\psi' \\ -\sin(\psi) - f_w'\,\phi\cos(\psi) & 1 + \Delta' - X\cos(\psi)\,\psi' - f_w\,\phi'\cos(\psi) + f_w\,\phi\sin(\psi)\,\psi' \end{pmatrix} \tag{8}$$

The determinant of the deformation gradient $J = \det(\mathbf{F})$ providing the ratio dv/dV of a differential volume in the deformed and reference configurations is given by:

$$J = (1+\Delta')\left[\cos(\psi) - f_w'\,\phi\sin(\psi)\right] + v'\left[\sin(\psi) + f_w'\,\phi\cos(\psi)\right] - X\psi' - f_w\,\phi' - f_w'\,f_w\,\phi^2\,\psi' \tag{9}$$

For subsequent analysis it will also be necessary to make use of the right Cauchy-Green deformation tensor $\mathbf{C} = \mathbf{F}^\top\mathbf{F}$ and the Green-Lagrange strain tensor $\mathbf{E} = (\mathbf{C} - \mathbf{I})/2$. By definition, the shear component of $\mathbf{E}$ is given by $2E_{12} = C_{12} = \mathbf{F}\mathbf{E}_1 \cdot \mathbf{F}\mathbf{E}_2$, such that:

$$2E_{12} = -(1+\Delta')\left[\sin(\psi) + f_w'\,\phi\cos(\psi)\right] + v'\left[\cos(\psi) - f_w'\,\phi\sin(\psi)\right] + X\psi' f_w'\,\phi - f_w\,\phi\,\psi' + f_w'\,f_w\,\phi'\,\phi \tag{10}$$

Next we define the unit vectors $\mathbf{L}$ and $\mathbf{N}$, tangent and normal to the cross section in the reference configuration, respectively, such that $\mathbf{L} = \mathbf{E}_1$ and $\mathbf{N} = \mathbf{E}_2$ (see Fig. 1). We can also define the unit vectors $\mathbf{l}$ and $\mathbf{n}$ tangent and normal to the cross section in the deformed configuration (see Fig. 1). Making use of Nanson's formula for the normal vector $\mathbf{n}$ (Holzapfel 2000):

$$\mathbf{n} = \left(\frac{dA}{da}\right) J\,\mathbf{F}^{-\top}\mathbf{N} = \left(\frac{dA}{da}\right)\left\{\left[\sin(\psi) + f_w'\,\phi\cos(\psi)\right]\mathbf{e}_1 + \left[\cos(\psi) - f_w'\,\phi\sin(\psi)\right]\mathbf{e}_2\right\} \tag{11}$$

where

$$\frac{da}{dA} = \|\mathbf{F}\mathbf{L}\| = \sqrt{1 + (f_w'\,\phi)^2} \tag{12}$$

is the ratio of a differential area in the deformed and reference configurations. Then, the tangent vector $\mathbf{l}$ is calculated as:

$$\mathbf{l} = \frac{\mathbf{FL}}{||\mathbf{FL}||} = \left(\frac{dA}{da}\right)\left\{\left[\cos(\psi) - f_w' \,\phi \sin(\psi)\right] \mathbf{e}_1 - \left[\sin(\psi) + f_w' \,\phi \cos(\psi)\right] \mathbf{e}_2\right\} \tag{13}$$

Lastly, consider a material curve $\hat{\boldsymbol{X}}(S) \in \mathcal{B}$, parameterized by S and direction given by the unit vector $\mathbf{M}$ such that its tangent $\hat{\boldsymbol{X}}'(S)$ is given by $\mathbf{M}dS$. The spatial form of the curve is given by $\boldsymbol{\varphi}(\hat{\boldsymbol{X}})$, and its tangent $\boldsymbol{\varphi}'(\hat{\boldsymbol{X}})$ corresponds to $\mathbf{m}ds$, with $\mathbf{m}$ a unit vector. The deformation gradient $\mathbf{F}$ can be used to obtain the stretch $\lambda = ds/dS$ of the spatial curve by $\lambda\mathbf{m} = \mathbf{FM}$. Then, making use of the definition of the unit vector $\mathbf{n}$ [Eq. (11)], we can define the following stretch:

$$\lambda_n = \mathbf{n} \cdot \mathbf{FN} = \left(\frac{dA}{da}\right) J \tag{14}$$

which corresponds to the stretch of a spatial curve that is normal to the beam's cross section in the reference configuration, in the direction normal to the deformed cross section.

Stress Measure

The physically meaningful stresses of force per unit area in the deformed configuration σ and τ, acting normal and tangent to the deformed cross section, will be used subsequently. It will be considered that the appropriate material constitutive relation is that which assumes linearity of σ and τ with respect to their conjugate strain measures, which will be derived later based on stress power considerations. This derives from the ideas presented by Simo (1982) in the context of the formulation of a geometrically exact rod theory that allows for shear deformation, but not warping. There, the generalized stresses resulting from the integration of σ and τ over the cross section were assumed to be linear with respect to their conjugate generalized strains. The consistent linearization of the resulting theory for an inextensible rod was shown to match with that of Haringx.

To obtain these stresses, we first define the two-point first Piola-Kirchhoff stress tensor $\mathbf{P} = \mathbf{p}_A \otimes \mathbf{E}_A$, where $\mathbf{p}_A$ is the traction vector of force per unit area in the reference configuration acting on a surface with unit vector $\mathbf{E}_A$. Thus, the traction vector acting on a differential area of the cross section is given by $\mathbf{p}_2 = \mathbf{PN}$. The traction vector acting on a differential area of the cross section in the deformed configuration then corresponds to $\mathbf{t}_n = (dA/da)\mathbf{p}_2$, and allows for the representation $\mathbf{t}_n = \tau\mathbf{l} + \sigma\mathbf{n}$. Hence, σ and τ can be obtained by:

$$\sigma = \left(\frac{dA}{da}\right)\mathbf{P} : (\mathbf{n} \otimes \mathbf{N}) = \left(\frac{dA}{da}\right)\mathbf{n} \cdot \mathbf{p}_2 \qquad \tau = \left(\frac{dA}{da}\right)\mathbf{P} : (\mathbf{l} \otimes \mathbf{N}) = \left(\frac{dA}{da}\right)\mathbf{l} \cdot \mathbf{p}_2 \tag{15}$$

Relations can be established between the stresses σ and τ and the components of the referential second Piola-Kirchhoff stress tensor $\mathbf{S}$, which are necessary for the derivation of the beam theory. Making use of the definition of the stress σ [Eq. (15)], the normal vector $\mathbf{n}$ [Eq. (11)], and the relation between stress tensors $\mathbf{P} = \mathbf{FS}$, we have $\sigma = (dA/da)^2 J\mathbf{F}^{-\top}\mathbf{E}_2 \cdot \mathbf{FSE}_2$ such that:

$$S_{22} = \left(\frac{da}{dA}\right)^2 \frac{\sigma}{J} \tag{16}$$

Using the definition of τ [Eq. (15)], the tangent vector $\mathbf{l}$ [Eq. (13)], and $\mathbf{P} = \mathbf{FS}$, we have $\tau = (\mathbf{FE}_1/||\mathbf{FE}_1||^2) \cdot \mathbf{FSE}_2$. Moreover, using the definition of the right Cauchy-Green deformation tensor $\mathbf{C}$, the Green-Lagrange strain tensor $\mathbf{E}$, and Eq. (16), we obtain:

$$S_{12} = \tau - 2E_{12}\frac{\sigma}{J} \tag{17}$$

Material Constitutive Relation

To formulate an appropriate constitutive relation for the stresses σ and τ we calculate the stress power $\mathcal{P}_{int}$ of the beam for the assumed deformation field:

$$\mathcal{P}_{int} = \int_{\mathcal{B}} \mathbf{P} : \dot{\mathbf{F}}\, dV \tag{18}$$

Employing the definition of $\mathbf{F}$ given in Eq. (8), this can be expanded as follows:

$$\begin{aligned}\mathcal{P}_{int} = &\int_0^h \dot{\Delta}' \int_{\mathcal{A}} \mathbf{p}_2 \cdot \mathbf{e}_2\, dA\, dZ + \int_0^h \dot{v}' \int_{\mathcal{A}} \mathbf{p}_2 \cdot \mathbf{e}_1\, dA\, dZ - \int_0^h \dot{\psi}' \int_{\mathcal{A}} [(\boldsymbol{\varphi} - \boldsymbol{\varphi}_o) \times \mathbf{p}_2] \cdot \mathbf{e}_3\, dA\, dZ \\ &+ \int_0^h \dot{\psi} \int_{\mathcal{A}} \Big\{ -(da/dA)\,\mathbf{n} \cdot \mathbf{p}_1 + [(-X\psi' - f_w\,\phi')\mathbf{d}_1 + f_w\,\phi\,\psi'\mathbf{d}_2] \cdot \mathbf{p}_2 \Big\}\, dA\, dZ\end{aligned} \tag{19}$$

$$+ \int_0^h \dot{\phi} \int_{\mathcal{A}} (-f_w' \, \mathbf{d}_2 \cdot \mathbf{p}_1 - f_w \, \psi' \mathbf{d}_1 \cdot \mathbf{p}_2) \; dA \, dZ + \int_0^h \dot{\phi}' \int_{\mathcal{A}} -f_w \, \mathbf{d}_2 \cdot \mathbf{p}_2 \, dA \, dZ$$

where the definitions of the traction vectors $\mathbf{p}_A$, directors $\mathbf{d}_i$ [Eq. (4)], the deformation $\boldsymbol{\varphi}$ [Eq. (2)], and the deformation of the beam's axis $\boldsymbol{\varphi}_o$ [Eq. (3)] have been used.

The resulting stress power can be expanded as:

$$\begin{aligned}
\mathcal{P}_{int} = & \int_0^h \dot{\Delta}' \int_{\mathcal{A}} \Big\{ \sigma \left[\cos(\psi) - f_w' \, \phi \sin(\psi) \right] + \tau \left[-\sin(\psi) - f_w' \, \phi \cos(\psi) \right] \Big\} \, dA \, dZ \\
& + \int_0^h \dot{v}' \int_{\mathcal{A}} \Big\{ \sigma \left[\sin(\psi) + f_w' \, \phi \cos(\psi) \right] + \tau \left[\cos(\psi) - f_w' \, \phi \sin(\psi) \right] \Big\} \, dA \, dZ \\
& + \int_0^h \dot{\psi} \int_{\mathcal{A}} \sigma \left(2E_{12} - X\psi' f_w' \, \phi - f_w' \, f_w \, \phi' \, \phi + f_w \, \phi \, \psi' \right) \, dA \, dZ \\
& + \int_0^h \dot{\psi} \int_{\mathcal{A}} \tau \left(-J - X\psi' - f_w \, \phi' - f_w' \, f_w \, \phi^2 \, \psi' \right) \, dA \, dZ \\
& + \int_0^h \dot{\psi}' \int_{\mathcal{A}} \left[\sigma \left(-X - f_w' \, f_w \, \phi^2 \right) + \tau \left(-f_w \, \phi + X f_w' \, \phi \right) \right] \, dA \, dZ \\
& + \int_0^h \dot{\phi} \int_{\mathcal{A}} \frac{\sigma}{J} \Big\{ 2E_{12} f_w' \left[(1 + \Delta') \cos(\psi) + v' \sin(\psi) - X\psi' - f_w \, \phi' \right] - f_w \, \phi \, \psi' \Big\} \, dA \, dZ \\
& + \int_0^h \dot{\phi} \int_{\mathcal{A}} \tau \left[-\left(1 + \Delta'\right) f_w' \, \cos(\psi) - v' f_w' \, \sin(\psi) + X\psi' f_w' + f_w' \, f_w \, \phi' - f_w \, \psi' \right] \, dA \, dZ \\
& + \int_0^h \dot{\phi} \int_{\mathcal{A}} \frac{\sigma_T}{J} \left(\frac{da}{dA} \right)^2 (f_w')^2 \phi \, dA \, dZ + \int_0^h \dot{\phi}' \int_{\mathcal{A}} \left(-\sigma f_w + \tau f_w' \, f_w \, \phi \right) \, dA \, dZ
\end{aligned} \tag{20}$$

where the normal stress σ_T perpendicular to the beam's axis in the reference configuration has been introduced, by means of a transformation of the second Piola-Kirchhoff stress component S_{11} equivalent to that presented in Eq. (16) for S_{22}. Moreover, the symmetry of the second Piola-Kirchhoff stress tensor $\mathbf{S}$ has also been exploited to establish $S_{12} = S_{21}$.

To proceed, we neglect the contribution of σ_T which allows us to keep the analysis one dimensional. Moreover, we recall that the rotation $f_w' \, \phi$ is related to the extension of the cross section as shown in Eq. (12). Thus, a large warping deformation would lead to a large change in cross-sectional area, which is not necessarily realistic but a by-product of the assumed deformation field which is an incomplete representation of the three-dimensional deformation. Therefore, we consider $f_w'\phi \ll 1$, hence $da/dA \approx 1$. Then, the stress power can be approximated by:

$$
\begin{aligned}
\mathcal{P}_{int} \approx & \int_0^h \dot{\Delta}' \int_{\mathcal{A}} \sigma\left[\cos(\psi) - f_w'\,\phi\sin(\psi)\right] + \tau\left[-\sin(\psi) - f_w'\,\phi\cos(\psi)\right]\, dA\, dZ \\
& + \int_0^h \dot{v}' \int_{\mathcal{A}} \sigma\left[\sin(\psi) + f_w'\,\phi\cos(\psi)\right] + \tau\left[\cos(\psi) - f_w'\,\phi\sin(\psi)\right]\, dA\, dZ \\
& + \int_0^h \dot{\psi} \int_{\mathcal{A}} \sigma\Big\{(1+\Delta')\left[-\sin(\psi) - f_w'\,\phi\cos(\psi)\right] + v'\left[\cos(\psi) - f_w'\,\phi\sin(\psi)\right]\Big\}\, dA\, dZ \\
& + \int_0^h \dot{\psi} \int_{\mathcal{A}} \tau\Big\{(1+\Delta')\left[-\cos(\psi) + f_w'\,\phi\sin(\psi)\right] + v'\left[-\sin(\psi) - f_w'\,\phi\cos(\psi)\right]\Big\}\, dA\, dZ \\
& + \int_0^h \dot{\psi}' \int_{\mathcal{A}} \sigma\left(-X - f_w'\,f_w\,\phi^2\right) - \tau\left(f_w\,\phi - X f_w'\,\phi\right)\, dA\, dZ \\
& + \int_0^h \dot{\phi} \int_{\mathcal{A}} \sigma\Big\{\left[-(1+\Delta')\,f_w'\,\sin(\psi) + v' f_w'\cos(\psi) - 2 f_w'\,f_w\,\phi\,\psi'\right] - J(f_w')^2\phi\Big\}\, dA\, dZ \\
& + \int_0^h \dot{\phi} \int_{\mathcal{A}} \tau\left[-(1+\Delta')\,f_w'\cos(\psi) - v' f_w'\sin(\psi) + X\psi'\,f_w' + f_w'\,f_w\,\phi' - f_w\,\psi'\right]\, dA\, dZ \\
& + \int_0^h \dot{\phi}' \int_{\mathcal{A}} \left(-\sigma f_w + \tau f_w'\,f_w\,\phi\right)\, dA\, dZ
\end{aligned}
\tag{21}
$$

which differs from the complete expression in Eq. (20) only by higher-order terms in $f_w'\phi$.

Let us define now the two strain measures:

$$
\epsilon = \lambda_n - 1 = \left(\frac{dA}{da}\right) J - 1 \qquad \Gamma = 2E_{12} \tag{22}
$$

Making use of Eq. (14), and using a second-order approximation for dA/da [Eq. (12)], we obtain:

$$
\begin{aligned}
\epsilon = & \left[1 - \frac{(f_w'\,\phi)^2}{2}\right]\Big\{(1+\Delta')\left[\cos(\psi) - f_w'\,\phi\sin(\psi)\right] \\
& + v'\left[\sin(\psi) + f_w'\,\phi\cos(\psi)\right] - X\psi' - f_w\,\phi' - f_w'\,f_w\,\phi^2\psi'\Big\} - 1
\end{aligned}
\tag{23}
$$

Also, recalling the expression for E_{12} [Eq. (10)], the stress power can be expressed as:

$$
\mathcal{P}_{int} \approx \int_0^h \int_{\mathcal{A}} \left(\sigma\dot{\epsilon} + \tau\dot{\Gamma}\right)\, dA\, dZ \tag{24}
$$

Note that second-order terms in $f_w'\,\phi$ in the definition of ϵ have been preserved because they contribute first-order terms in $f'_w \phi$ to $\mathcal{P}_{int}$. The previous expression leads to the work conjugacy between σ and ϵ, and τ and Γ when $f'_w \phi$ is small. Notice that for the problem without warping $\phi = 0$ and $da/dA = 1$, rendering the previous expression for the stress power exact. This can be interpreted from the work by Reissner (1972) and Simo (1982), albeit those formulations were established directly in terms of generalized stresses and strains.

For the purely mechanical theory and a perfectly elastic material, hyperelasticity assumes the existence of a strain-energy function W per unit volume, such that $\dot{W} = \mathbf{P} : \dot{\mathbf{F}}$. For our case, this leads to $\dot{W} = \sigma\dot{\epsilon} + \tau\dot{\Gamma}$, resulting in:

$$W = \hat{W}(\epsilon, \Gamma) \qquad \sigma = \frac{\partial \hat{W}(\epsilon, \Gamma)}{\partial \epsilon} \qquad \tau = \frac{\partial \hat{W}(\epsilon, \Gamma)}{\partial \Gamma} \tag{25}$$

The simplest model that can be assumed corresponds to a quadratic function in ϵ and Γ:

$$W = \frac{E\epsilon^2}{2} + \frac{G\Gamma^2}{2} \tag{26}$$

where E and G are equivalent to the Young's modulus and shear modulus of the infinitesimal elasticity theory. Then, the stresses σ and τ are linear functions of their conjugate strain measures:

$$\sigma = E\epsilon \qquad \tau = G\Gamma \tag{27}$$

Making use of the displacement gradient $\mathbf{H} = \partial\mathbf{u}/\partial\mathbf{X}$ where $\mathbf{u} = \boldsymbol{\varphi} - \mathbf{X}$, the linearization of the strains ϵ and Γ [Eq. (22)] with respect to the undeformed configuration can be shown to be:

$$\mathrm{L}[\epsilon]_{\boldsymbol{\eta}=\mathbf{0}} = H_{22} = \varepsilon_z \qquad \mathrm{L}[\Gamma]_{\boldsymbol{\eta}=\mathbf{0}} = H_{12} + H_{21} = \gamma_{xz} \tag{28}$$

where ε_z and γ_{xz} are the engineering strains of the infinitesimal theory. Hence, the linearized material model coincides with the one-dimensional case from linear elasticity, as should be expected.

Variational Formulation

To derive the stability condition for the equilibrium of the beam subjected to a compressive axial load P, we start by defining the potential energy Π:

$$\Pi = \int_{\mathcal{B}} W dV + \Pi_{ext} \tag{29}$$

where W is defined in Eq. (26) and Π_{ext} is the potential due to external loads. The equilibrium state is obtained following the principle of stationary potential energy:

$$\delta\Pi = \int_{\mathcal{B}} (\sigma\delta\epsilon + \tau\delta\Gamma) dV + \delta\Pi_{ext} = 0 \tag{30}$$

This expression simply corresponds to the material description of the principle of virtual work, the weak form of the balance of linear momentum in the reference configuration. Since time derivatives and variations of scalar fields behave in the same way, the expansion of the internal virtual work is analogous to Eq. (21), replacing the time derivatives $(\dot{\bullet})$ with variations $\delta(\bullet)$.

According to the Lagrange-Dirichlet energy criterion, an equilibrium state of a conservative system is stable when it corresponds to a minimum of the potential energy such that $\delta^2\Pi > 0$, whereas a critical state of equilibrium is associated with $\delta^2\Pi = 0$ (Bažant and Cedolin 2010). Thus, the critical state of interest can be obtained by linearizing $\delta\Pi$ with respect to the equilibrium state corresponding to the beam subjected to P, which causes an axial stress σ_o such that $-\int_{\mathcal{A}} \sigma_o = P$, an axial displacement Δ_o and the axial strain Δ'_o, while $\tau_o = v_o = \psi_o = \phi_o = 0$:

$$\begin{aligned}
d\delta\Pi = & \int_0^h \delta\Delta' \int_{\mathcal{A}} d\sigma \, dA \, dZ + \int_0^h \delta v' \int_{\mathcal{A}} \left[\sigma_o \left(d\psi + f'_w \, d\phi\right) + d\tau\right] dA \, dZ \\
& + \int_0^h \delta\psi \int_{\mathcal{A}} \left\{\sigma_o \left[(1+\Delta'_o)\left(-d\psi - f'_w \, d\phi\right) + dv'\right] - d\tau \left(1+\Delta'_o\right)\right\} dA \, dZ \\
& + \int_0^h \delta\phi \int_{\mathcal{A}} \left\{\sigma_o \left\{(1+\Delta'_o)\left[-f'_w \, d\psi - (f'_w)^2 d\phi\right] + f'_w \, dv'\right\} - d\tau \left(1+\Delta'_o\right) f'_w\right\} dA \, dZ \\
& + \int_0^h \delta\psi' \int_{\mathcal{A}} -X d\sigma \, dA \, dZ + \int_0^h \delta\phi' \int_{\mathcal{A}} -f_w \, d\sigma \, dA \, dZ = 0
\end{aligned} \tag{31}$$

Linearizing Eqs. (23) and (10) accordingly, the incremental stresses $d\sigma$ and $d\tau$ are given by:

$$d\sigma = E\left(d\Delta' - Xd\psi' - f_w d\phi'\right) \qquad d\tau = G\left[dv' - (1+\Delta_o')\left(d\psi + f_w'\, d\phi\right)\right] \tag{32}$$

In the following, the notation $d(\bullet)$ is dropped to simplify the expressions. It should be recalled, however, that the strains and stresses are incremental, coming from the linearization of the principle of virtual work. Moreover, we define the following stress resultants:

$$\begin{aligned}
P &= -\int_{\mathcal{A}} \sigma_o\, dA = -EA\Delta_o' && N = \int_{\mathcal{A}} \sigma\, dA = EA\Delta' \\
M &= -\int_{\mathcal{A}} X\sigma\, dA = EI\psi' && V = \int_{\mathcal{A}} \tau\, dA = GA\left[v' - (1+\Delta_o')\left(\psi + \frac{GB}{GA}\phi\right)\right] \\
Q &= -\int_{\mathcal{A}} f_w\, \sigma\, dA = EJ\phi' && R = \int_{\mathcal{A}} f_w'\, \tau\, dA = GB\left[v' - (1+\Delta_o')\left(\psi + \frac{GC}{GB}\phi\right)\right]
\end{aligned} \tag{33}$$

with the corresponding cross-sectional rigidities and properties:

$$\begin{gathered}
EA = \int_{\mathcal{A}} E dA \qquad EI = \int_{\mathcal{A}} EX^2\, dA \qquad EJ = \int_{\mathcal{A}} Ef_w^2\, dA \\
GA = \int_{\mathcal{A}} G dA \qquad GB = \int_{\mathcal{A}} Gf_w'\, dA \qquad GC = \int_{\mathcal{A}} G(f_w')^2 dA \\
f_B = -\frac{\int_{\mathcal{A}} f_w'\, \sigma_o\, dA}{P/A} \qquad f_C = -\frac{\int_{\mathcal{A}} (f_w')^2 \sigma_o\, dA}{P/A}
\end{gathered} \tag{34}$$

where the modulus-weighted centroidal location of the beam's axis ($\int_{\mathcal{A}} EXdA = 0$) and conditions in Eq. (5) for f_w have been used. The resultants Q and R correspond to the warping moment and shear, respectively. The term EJ is the warping rigidity, while GB and GC are warping-related shear rigidities with the same dimensions as GA. For a homogeneous element, the shear modulus G and the initial axial stress σ_o are uniform, hence $f_B = B = \int_{\mathcal{A}} f_w' dA$ and $f_C = C = \int_{\mathcal{A}} (f_w')^2 dA$. However, for non-homogeneous elements, such as elastomeric bearings, these properties differ. The rest of resultants and cross-sectional rigidities are interpreted in the standard way.

The linearization of the principle of virtual work is then restated as follows in terms of generalized stress resultants:

$$d\delta\Pi = \int_0^h \left\{ \delta\Delta' N - \delta v' \left[P\left(\psi + \frac{f_B}{A}\phi\right) - V \right] + \delta\psi' M + \delta\phi' Q \right\} dZ$$
$$- \int_0^h \delta\psi \left\{ P\left[v' - (1+\Delta_o')\left(\psi + \frac{f_B}{A}\phi\right) \right] + V(1+\Delta_o') \right\} dZ \tag{35}$$
$$- \int_0^h \delta\phi \left\{ P\frac{f_B}{A}\left[v' - (1+\Delta_o')\left(\psi + \frac{f_C}{f_B}\phi\right) \right] + R(1+\Delta_o') \right\} dZ = 0$$

Using integration by parts, neglecting the incremental axial load N which is trivially zero, and using the definitions in Eq. (33), the strong form of the buckling eigenvalue problem becomes:

$$P\left(\psi' + \frac{f_B}{A}\phi'\right) - GA\left[v'' - (1+\Delta_o')\left(\psi' + \frac{GB}{GA}\phi'\right) \right] = 0 \tag{36a}$$

$$EI\psi'' + P\left[v' - (1+\Delta_o')\left(\psi + \frac{f_B}{A}\phi\right) \right] + GA\left[v' - (1+\Delta_o')\left(\psi + \frac{GB}{GA}\phi\right) \right](1+\Delta_o') = 0 \tag{36b}$$

$$EJ\phi'' + P\frac{f_B}{A}\left[v' - (1+\Delta_o')\left(\psi + \frac{f_C}{f_B}\phi\right) \right] + GB\left[v' - (1+\Delta_o')\left(\psi + \frac{GC}{GB}\phi\right) \right](1+\Delta_o') = 0 \tag{36c}$$

with the boundary terms:

$$\left\{ \left\{ GA\left[v' - (1+\Delta_o')\left(\psi + \frac{GB}{GA}\phi\right) \right] - P\left(\psi + \frac{f_B}{A}\phi\right) \right\} \delta v \right\}\Big|_0^h + (EI\psi'\delta\psi)\Big|_0^h + (EJ\phi'\delta\phi)\Big|_0^h = 0 \tag{37}$$

If the element is very stiff in compression, such that the initial axial strain Δ_o' can be neglected, these equations coincide with those of the Kelly-Tsai theory.

The previous equations can be interpreted as the equilibrium equations corresponding to the deformed configuration shown in Fig. 2. As opposed to Haringx's theory, where the axial load acts perpendicular to the deformed cross section, in this case the line of action of P has an additional rotation of $\phi f_B/A$ with respect to the normal to the average cross-sectional plane in the deformed configuration. Equation (36a) then corresponds to the equilibrium of forces in X, while Eq. (36b) corresponds to the moment equilibrium. The cross-sectional distortion leads to additional stresses with no resultant force or moment, according to the requirements in Eq. (5). Equation (36c) establishes the equilibrium of these stresses in terms of the higher-order warping moment Q and shear R, which cannot be interpreted as moments or forces in the standard sense.

Buckling Load Equation

The critical load of a beam with fixed lateral displacement at its base, and fixed rotation and warping at both ends is estimated next; these correspond to the standard conditions for elastomeric bearings used for seismic base isolation with flexurally rigid supports. Hence, the essential boundary conditions are $v(0) = \psi(0) = \phi(0) = \psi(h) = \phi(h) = 0$, while the natural boundary condition is $V(h) = 0$. In other applications including bridges and mid-height isolation, support rotation can have important effects, as illustrated by Moghadam and Konstantinidis (2017, 2021), and should be considered. The procedure outlined next can be followed to estimate P_{cr} for those cases by enforcing non-vanishing rotations $\psi(0)$ and/or $\psi(h)$. For unbonded isolators, this approach will be valid for small to moderate rotations for which the whole cross section remains in contact with the supports; for large rotations, lift-off might occur (Konstantinidis et al. 2008; Stanton et al. 2008; Van Engelen 2019b), and the present approach will not be readily applicable in those instances.

The buckling load of the beam comes from solving the system of ordinary differential equations in Eq. (36). Integrating Eq. (36a) and making use of the normalized axial load $\bar{P} = P/GA$ we obtain:

$$v' = \left(\bar{P} + \lambda_o\right)\psi + \left(\bar{P}\,\frac{f_B}{A} + \lambda_o\,\frac{GB}{GA}\right)\phi \tag{38}$$

where $\lambda_o(\bar{P}) = 1 + \Delta_o'(\bar{P})$ is the initial stretch of the element given by:

$$\lambda_o(\bar{P}) = 1 - \bar{P}\,\frac{GA}{EA} \tag{39}$$

Substituting this in Eqs. (36b) and (36c), we get:

$$\phi = -\frac{1}{\bar{P}\left(\bar{P}\,\frac{f_B}{A} + \lambda_o\,\frac{GB}{GA}\right)}\left[\frac{EI}{GA}\,\psi'' + \bar{P}\left(\bar{P} + \lambda_o\right)\psi\right] \tag{40}$$

$$\psi = -\frac{1}{\bar{P}\left(\bar{P}\,\frac{f_B}{A} + \lambda_o\,\frac{GB}{GA}\right)}\left\{\frac{EJ}{GA}\,\phi'' + \left[\left(\bar{P}\,\frac{f_B}{A} + \lambda_o\,\frac{GB}{GA}\right)^2 - \lambda_o\left(\bar{P}\,\frac{f_C}{A} + \lambda_o\,\frac{GC}{GA}\right)\right]\phi\right\} \tag{41}$$

Substituting Eq. (40) in Eq. (41), the differential equation for $\psi(Z)$ becomes:

$$\psi^{iv} + \frac{\bar{P}\left(\bar{P}+\lambda_o\right)+\kappa_B-\kappa_C}{\Omega h^2}\,\psi'' - \frac{\bar{P}\left[\left(\bar{P}+\lambda_o\right)\kappa_C-\lambda_o\kappa_B\right]}{\Omega^2 h^4}\,\psi = 0 \tag{42}$$

where we have used $\Omega = EI/GAh^2$ and the following non-dimensional parameters:

$$\kappa_B(\bar{P}) = \left(\bar{P}\,\frac{f_B}{A}+\lambda_o\,\frac{GB}{GA}\right)^2\frac{EI}{EJ} \qquad \kappa_C(\bar{P}) = \lambda_o\left(\bar{P}\,\frac{f_C}{A}+\lambda_o\,\frac{GC}{GA}\right)\frac{EI}{EJ} \tag{43}$$

The solution to Eq. (42) is given by:

$$\psi(Z) = A\cos(\beta_1 Z) + B\sin(\beta_1 Z) + C\cosh(\beta_2 Z) + D\sinh(\beta_2 Z) \tag{44a}$$

$$\beta_1^2 = \frac{1}{2\Omega h^2}\left\{\left[\bar{P}\left(\bar{P}+\lambda_o\right)+\kappa_B-\kappa_C\right] + \sqrt{\left[\bar{P}\left(\bar{P}+\lambda_o\right)+\kappa_B-\kappa_C\right]^2+4\bar{P}\left[\left(\bar{P}+\lambda_o\right)\kappa_C-\lambda_o\kappa_B\right]}\right\} \tag{44b}$$

$$\beta_2^2 = \frac{-1}{2\Omega h^2}\left\{\left[\bar{P}\left(\bar{P}+\lambda_o\right)+\kappa_B-\kappa_C\right] + \sqrt{\left[\bar{P}\left(\bar{P}+\lambda_o\right)+\kappa_B-\kappa_C\right]^2+4\bar{P}\left[\left(\bar{P}+\lambda_o\right)\kappa_C-\lambda_o\kappa_B\right]}\right\} \tag{44c}$$

The solution to the system of equations using the boundary conditions yields either the trivial solution $A = B = C = D = 0$, or the solution $\beta_1 h = \pi$. The latter, upon expansion, results in:

$$\bar{P}\left\{\left[\bar{P}+\lambda_o(\bar{P})\right]\kappa_C(\bar{P}) - \lambda_o(\bar{P})\,\kappa_B(\bar{P})\right\} + \pi^2\Omega\left\{\bar{P}\left[\bar{P}+\lambda_o(\bar{P})\right]+\kappa_B(\bar{P})-\kappa_C(\bar{P})\right\} - \pi^4\Omega^2 = 0 \tag{45}$$

where the functional dependence of λ_o, κ_B and κ_C on $\bar{P}$ has been explicitly stated for clarity. This corresponds to a quartic equation on $\bar{P}$, whose solution yields the normalized buckling load $\bar{P}_{cr}$. This equation can be solved by appropriate numerical procedures such as Newton's method. To ensure the convergence of the solution method, a good initial search value is required. This can be given by an approximation of Haringx's buckling load for $P_E \gg P_S$ (also $\Omega \to \infty$) [see Eq. (1)]:

$$P_{cr}^{(0)} = \sqrt{P_S P_E} \tag{46}$$

where the superscript indicates the iteration of the numerical procedure.

Equation (45) provides the exact result for the developments presented here. However, the complexity of the solution to a quartic equation makes its implementation impractical in the context of design applications. If the axial shortening caused by the buckling load is neglected, such that $\lambda_o = 1$, the cubic equation from the Kelly-Tsai theory is recovered; yet, its solution remains onerous. The present formulation is of particular interest for short composite elements which are soft in shear. In those cases, the axial-to-shear stiffness ratio, EA/GA, and the bending-to-shear stiffness ratio, $\Omega = EI/GAh^2$, can acquire large values. For example, in elastomeric isolators with moderate-to-high shape factor EA/GA is in the range of 100-10,000, while Ω is in the range of 10-10,000. Fig. 3 shows that in those instances the solution of Eq. (45) converges to:

$$P_{cr} \approx \sqrt{\frac{P_S P_E}{1 + \left(\frac{f_B}{A}\right)^2 \frac{EI}{EJ}}} \tag{47}$$

which corresponds to a modification of Haringx's approximate load [Eq. (46)] based on the bending-to-warping rigidity ratio EI/EJ and the ratio f_B/A which measures the angular deviation of the line of action of P with respect to the normal to the average cross-sectional plane (see Fig. 2).

COMPARISON WITH OTHER FORMULATIONS

The present formulation has been derived by analyzing the geometrically nonlinear beam to establish an appropriate hyperelastic material assumption and allow for additional effects, such as axial shortening. Upon neglecting the latter effect, it coincides with the Kelly-Tsai theory. However, this theory differs significantly from that by Simo (1982), as well as other buckling theories that have been proposed for higher-order shear beams (Wang et al. 2000; Challamel 2011; Challamel et al. 2013). Thus, before applying this theory to elastomeric bearings, it is deemed necessary to explore the differences giving rise to distinct formulations. First, a second-order approximation of the potential energy is introduced for the present theory; Simo's theory and one of the solutions by Challamel (2011) are presented using such a potential energy. Then, the differences giving rise to distinct formulations are discussed. Finally, the theories are compared for the case of a homogeneous beam to illustrate their different behavior for short elements highly-flexible in shear.

Buckling Theories

Proposed theory

If the nonlinear material constitutive relation is known, only a linear displacement field and second-order approximations of the strain measures are required to determine the critical load. The linear displacement field associated with the present developments can be obtained by taking the linearization of the displacement field $\mathbf{u} = \boldsymbol{\varphi} - \mathbf{X}$ with respect to the undeformed configuration:

$$\mathrm{L}[\mathbf{u}]_{\boldsymbol{\eta}=\mathbf{0}} = v\mathbf{e}_1 + (\Delta - X\psi - f_w\,\phi)\,\mathbf{e}_2 \tag{48}$$

This linear displacement field coincides with that assumed in the Kelly-Tsai theory.

Moreover, it is convenient to state a second-order approximation of the potential energy directly in terms of the cross-sectional rigidities and generalized strains. Such a potential, which can be employed to derive the equilibrium equations in a more direct way, is given by:

$$\Pi(v,\psi,\phi) = \frac{1}{2}\int_0^h \begin{Bmatrix}\psi' \\ \phi' \\ \tilde{\gamma} \\ \tilde{\phi}\end{Bmatrix}^{\mathsf{T}} \begin{pmatrix} EI & 0 & 0 & 0 \\ 0 & EJ & 0 & 0 \\ 0 & 0 & GA + \tilde{P} & -GB - \tilde{P}\,\frac{f_B}{A} \\ 0 & 0 & -GB - \tilde{P}\,\frac{f_B}{A} & GC + \tilde{P}\,\frac{f_C}{A} \end{pmatrix} \begin{Bmatrix}\psi' \\ \phi' \\ \tilde{\gamma} \\ \tilde{\phi}\end{Bmatrix} - \tilde{P}(v')^2\,dZ \tag{49}$$

where $\tilde{\gamma} = v' - (1 + \Delta_o')\psi$, $\tilde{\phi} = (1 + \Delta_o')\phi$ and $\tilde{P} = P/(1 + \Delta_o')$. Recall that $f_B = B$ and $f_C = C$, respectively, for elements with homogeneous materials.

Simo's theory

Simo derived the beam's deformation field based on the solution of the boundary value problem of a sheared planar bearing which enforces compatibility between the deformation of the reinforcement and that of the rubber, with the only kinematic assumption that the lateral displacement v is only a function of the axial coordinate Z. The resulting displacement is equivalent to that of Eq. (48), with

$\phi = \bar{\gamma} = v' - \psi$. The warping function f_w depends on the stiffness of the reinforcing plate and when the reinforcement is fully flexible in bending, it is given by Eq. (7) with $\omega = -3/10$. Equilibrium was established based on the integration of a second-order approximation of the balance of linear momentum in referential form $\mathrm{Div}\,\mathbf{P} = \mathbf{0}$ over the cross section.

Alternatively, we can derive this formulation from the following potential energy:

$$\Pi^S(v, \psi, \phi, R) = \frac{1}{2}\int_0^h \begin{Bmatrix} \psi' \\ \tilde{\gamma} \\ \tilde{\phi} \end{Bmatrix}^{\mathsf{T}} \begin{pmatrix} EI & 0 & 0 \\ 0 & GA + \tilde{P} & -GB - \tilde{P}\,\frac{f_B}{A} \\ 0 & -GB - \tilde{P}\,\frac{f_B}{A} & GC + \tilde{P}\,\frac{f_C}{A} \end{pmatrix} \begin{Bmatrix} \psi' \\ \tilde{\gamma} \\ \tilde{\phi} \end{Bmatrix} - \tilde{P}(v')^2 + 2R\,(\bar{\gamma} - \phi)\; dZ \tag{50}$$

where the definitions of the cross-sectional rigidities are as before, but the warping shear R is now a Lagrange multiplier enforcing $\phi = \bar{\gamma}$. Taking admissible variations of the proposed potential, the system of differential equations defining the problem is:

$$P\left[\psi' + (1-\kappa)\,(v'' - \psi')\right] - \kappa GA\left[v'' - (1 + \Delta_o')\,\psi'\right] = 0 \tag{51a}$$

$$EI\psi'' + P\Big\{v' - (1 + \Delta_o')\left[\psi + (1-\kappa)\,(v' - \psi)\right]\Big\} + (1 + \Delta_o')\,\kappa GA\left[v' - (1 + \Delta_o')\,\psi\right] = 0 \tag{51b}$$

with boundary conditions given by:

$$\Big\{\left[\kappa GA\tilde{\gamma} - P\,(\psi + (1-\kappa)\,\tilde{\gamma})\right]\delta v\Big\}\Big|_0^h + \left(EI\psi'\delta\psi\right)\Big|_0^h = 0 \tag{52}$$

where $\kappa = 1 - 2GB/GA + GC/GA$. Then, inextensibility was assumed to obtain the following solution for the critical load for a beam fixed at the base, and with fixed rotation but free to displace at the top:

$$P_{cr}^S = \frac{2P_E}{1 + \frac{(1-\kappa)P_E}{\kappa GA} + \sqrt{\left[1 + \frac{(1-\kappa)P_E}{\kappa GA}\right]^2 + \frac{4P_E}{GA}}} \tag{53}$$

Alternative theories

Outside the realm of elastomeric bearings, the buckling of some higher-order shear beams has been studied. Wang et al. (2000) studied the buckling for the Bickford-Reddy beam (Bickford 1982; Reddy 1984), Challamel (2011) presented a buckling solution for the Shi-Voyiadjis beam (Shi and Voyiadjis 2010), and Challamel et al. (2013) derived and compared the critical loads for a large number of higher-order beam theories including those in (Bickford 1982; Touratier 1991; Karama et al. 2003; Shi and Voyiadjis 2010; El Meiche et al. 2011), all of which take the warping amplitude to be proportional to $\bar{\gamma}$ but differ in the definition of the warping function f_w. The buckling solution of the Shi-Voyiadjis beam, which assumes the same displacement field as Simo's theory, is presented next to illustrate the approach followed in these studies. The Engesser-type buckling theory, as referred to by Challamel (2011), was derived following a variational approach and will be referred to as Challamel's theory.

We can derive the equations from the following second-order potential:

$$\Pi^C(v,\psi,\phi,R) = \frac{1}{2}\int_0^h \begin{Bmatrix} \psi' \\ \phi' \\ \bar{\gamma} \\ \phi \end{Bmatrix}^{\mathsf{T}} \begin{pmatrix} EI & 0 & 0 & 0 \\ 0 & EJ & 0 & 0 \\ 0 & 0 & GA & -GB \\ 0 & 0 & -GB & GC \end{pmatrix} \begin{Bmatrix} \psi' \\ \phi' \\ \bar{\gamma} \\ \phi \end{Bmatrix} - P(v')^2 + 2R(\bar{\gamma}-\phi)\, dZ \tag{54}$$

where, again, the cross-sectional rigidities have been defined as before and the warping shear stress R is a Lagrange multiplier enforcing the warping amplitude to be equal to $\bar{\gamma}$. Taking admissible variations and integrating by parts, the system of equations to be solved is:

$$Pv'' - \kappa GA\,(v'' - \psi') + EJ\left(v^{iv} - \psi'''\right) = 0 \tag{55a}$$

$$EI\psi'' - EJ\,(v''' - \psi'') + \kappa GA\,(v' - \psi) = 0 \tag{55b}$$

with boundary conditions given by:

$$\left[(\kappa GA\bar{\gamma} - EJ\bar{\gamma}'' - Pv')\,\delta v\right]\Big|_0^h + \left[(EI\psi' - EJ\bar{\gamma}')\,\delta\psi\right]\Big|_0^h + (EJ\bar{\gamma}'\delta v')\Big|_0^h = 0 \tag{56}$$

where κ is as before. Then, the critical load for the boundary conditions of interest is:

$$P_{cr}^{C} = P_E\,\frac{1 + \frac{P_E}{\kappa GA}\frac{EJ}{EI}}{1 + \frac{P_E}{\kappa GA}\left(1 + \frac{EJ}{EI}\right)} \tag{57}$$

Theoretical Differences

For higher-order shear beams, several different buckling solutions can be derived on the basis of (1) the assumed deformation field, (2) the variational consistency of the equilibrium equations, and (3) the nonlinear material constitutive relation assumption. The first two items lead to differences in the linear beam theories for which, unlike the first-order shear case given by the Timoshenko beam theory, there is no consensus. The third item causes further differences in the nonlinear equations used for the estimation of the critical load. In the following, these aspects are discussed and the theories compared with respect to them.

Assumed displacement field

Two-aspects of the displacement can be altered: the warping function f_w and the warping amplitude ϕ. The definition of f_w has monopolized most of the discussion regarding higher-order shear beams (e.g., Bickford 1982; Touratier 1991; Karama et al. 2003; Shi and Voyiadjis 2010; El Meiche et al. 2011). However, as shown by Challamel et al. (2013), different warping functions lead to negligible differences in the buckling results. Moreover, the three formulations discussed make use of the same f_w and thus the discussion will focus on the warping amplitude. The vast majority of formulations take the warping amplitude to be $\phi = \bar{\gamma} = v' - \psi$, and this approach is followed by the kinematic assumptions in Simo's and Challamel's formulations. This is often argued to be in agreement with the displacement fields corresponding to the exact elasticity solutions for the problem of a beam subjected to transverse terminal loads (e.g., Simo 1982).

Such classical solutions, presented by Love (1944), can only satisfy traction boundary conditions at the ends of the element in a weak sense in terms of cross-sectional force and moment resultants, but not in a point-wise manner (Barber 2010). Hence, these solutions correspond to unrestrained warping cases where a cross-sectional distortion results even at clamped ends. When specific traction distributions or displacements are enforced at the beam's ends, additional self-equilibrated tractions will develop. Per Saint-Venant's principle, these tractions will be local and have negligible effects at large distances from the end. For elasticity problems, the classical stress field results require corrective solutions using eigenfunctions that decay exponentially away from the boundaries and modify the displacement field (Timoshenko and Goodier 1970; Barber 2010). Thus, exact elasticity solutions for the restrained warping problem do not satisfy $\phi = \bar{\gamma}$.

Taking $\phi = \bar{\gamma}$ should then be viewed as a constrained formulation, as illustrated by the derivation of Simo's and Challamel's theories presented herein. An analogous situation arises when dealing with the case of restrained torsional warping, as has been recently detailed by Armero (2022). This constraint allows to select f_w such that the shear stresses vanish at the top and bottom surfaces of the beam. Moreover, when inextensibility is assumed, a quadratic equation for the critical load is obtained, leading to a closed-form solution which is desirable for practical purposes. When ϕ is an independent kinematic variable, the shear stress depends on $\bar{\gamma}$ and ϕ, and the traction-free boundary condition at the top and bottom surfaces of the beam will not be satisfied. Thus, the theory might predict adequately the global response but not necessarily the local strain and stress distributions. Furthermore, even if inextensibility is assumed, a higher-order equation is obtained for the critical load whose closed-form solution is impractical, as shown in the Kelly-Tsai theory.

Variational consistency

The theories need to satisfy the variational principles of mechanics which, in the case of infinitesimal deformations of a one-dimensional element, read:

$$\delta\Pi = \int_{\mathcal{B}} (\sigma\delta\varepsilon + \tau\delta\gamma)\, dV + \delta\Pi_{ext} = 0 \tag{58}$$

This requirement, trivial in other contexts, has proved to be an issue in the derivations of higher-order beam and plate theories (Bickford 1982; Reddy 1984). Following a variational approach, the higher-order warping resultants Q and R [Eq. (33)] appear naturally. The present formulation and the Shi-Voyiadjis beam used for Challamel's buckling theory satisfy this requirement. In the latter theory, however, the higher-order shear R appears as a Lagrange multiplier due to the constrained nature of the formulation. Simo's theory neglects the higher-order warping moment contributions, hence violating variational consistency. It is remarked that Simo (1982) referred to his formulation as being *consistent* with the nonlinear balance principles of finite elasticity. However, his treatment of structural members (rods and plates) only accounted for equilibrium of forces and moments, whereas a balance of higher-order resultants is also necessary for cases with restrained warping. Thus, Simo's formulation is only valid for cases with unrestrained warping.

Material constitutive relation

The proposed theory is the only one, to the authors' knowledge, to rigorously establish the material relation at the stress-strain level [Eq. (26)] as an intrinsic part of the formulation for the case of elements that account for cross-sectional warping due to shear. The nonlinear equilibrium equations of the Kelly-Tsai theory were derived taking a second-order approximation of the extension of a differential element. The equations developed in the present study evidence that this agrees with the material constitutive relation presented herein up to second-order terms upon assuming inextensibility. In Simo's theory, no reference was made of a material relation at the stress-strain level, but linearity was assumed for the generalized stress resultants obtained from the integration of a second-order approximation of the referential form of the balance of linear momentum. Eq. (50) evidences the material constitutive relation embedded in this procedure to be analogous to the constitutive relation presented here, up to second-order terms.

The alternative formulations follow what their authors have deemed an Engesser approach, where the second-order contribution of the axial load to the potential energy is equivalent to that in Eq. (54) (Wang et al. 2000; Challamel 2011; Challamel et al. 2013). Engesser's theory for first-order shear beams has been explained by taking a Saint-Venant Kirchhoff material (see Holzapfel

2000) and neglecting all second-order terms except for $(v')^2/2$ in the axial component of the Green-Lagrange strain tensor E_{22} on the basis of rotations being larger than strains and $\sigma_{cr} \gg E$ (Bažant and Cedolin 2010). However, for the higher-order shear beam with displacement field given by Eq. (48) with $\phi = \bar{\gamma}$ we have:

$$E_{22} = \Delta' - X\psi' - f_w\,\phi' + \frac{1}{2}(v')^2 + \frac{1}{2}\left[\Delta' - X\psi' - f_w\,(v' - \psi)\right]^2 \tag{59}$$

The assumptions used for Engesser's theory do not justify neglecting some of the higher-order terms in E_{22}, and these theories cannot be directly traced back to any particular material model.

Comparison

The implications of the differences between theories are illustrated by means of two examples. The analysis is developed for the case of a planar beam with homogeneous material, such that $GB = GC = GA/6$, $\kappa = 5/6$ and $EJ = EI/84$. The calculations for the non-homogeneous elastomeric bearings are somewhat different because effective rigidities and cross-sectional parameters need to be employed, as will be shown in the next section. However, the qualitative behavior of the theories presented in the following remains the same.

Displacement under lateral load

The distinct kinematic assumptions and satisfaction of variational consistency lead to differences even in the linear equilibrium equations where axial load effects are neglected. This can be illustrated by estimating the lateral displacement of a beam with fixed ends, but allowed to move laterally at the top support upon the application of a lateral load H in the absence of an axial load P. For Simo's theory with variational inconsistency and constrained warping amplitude, only four boundary conditions are required in terms of v and ψ or their conjugate generalized forces [Eq. (52)]. A fixed end requires $v = \psi = 0$, but the cross-sectional warping does not vanish (Fig. 4a). The displacement at the top of the beam is given by:

$$v^S(h) = \frac{Hh^3}{12EI} + \frac{Hh}{\kappa GA} \tag{60}$$

which coincides with the classical solution for a beam with unrestrained warping.

In the absence of axial load, the present formulation is equivalent to the beam theory presented by Kelly (1994), and thus a superscript K will be used for reference. The variationally consistent theory with independent warping amplitude ϕ requires six boundary conditions to be enforced in terms of the generalized displacements v, ψ and ϕ or their conjugate generalized forces [Eq. (37)]. The enforcement of fixed boundary conditions requires $v = \psi = \phi = 0$ at that boundary, which is kinematically consistent (Fig. 4b). In this case, the solution is given by:

$$v^K(h) = \frac{Hh^3}{12EI} + \frac{Hh}{\kappa GA} + \frac{(1-\kappa)\,Hl^K}{\kappa GA}\left\{\operatorname{csch}\left(\frac{h}{l^K}\right)\left[\cosh\left(\frac{h}{l^K}\right) - 1\right]^2 - \sinh\left(\frac{h}{l^K}\right)\right\} \tag{61}$$

where $l^K = \sqrt{EJ/[(1-\kappa)\kappa GA]}$ corresponds to a characteristic length of the beam theory. The additional term in the solution appears due to the effect of restraining the warping deformation at the supports, and it reduces the lateral displacement of the beam.

Lastly, for a variationally consistent formulation with constrained warping amplitude, such as the Shi-Voyiadjis beam, six boundary conditions are again required but now in terms of v, v' and ψ [Eq. (56)]. For a fixed boundary condition, $v = v' = \psi = 0$, such that the cross-sectional distortion vanishes at the boundary. The shear stress, proportional to $\bar{\gamma}$ in this case, necessarily vanishes at the boundary as well (Fig. 4c). Thus an effective shear force conjugate to the lateral displacement v is needed [Eq. (56)], where the additional contribution comes from equilibrium but not from the integration of the shear stress over the cross section. This corresponds to an inconsistency arising from the constrained nature of the formulation. The lateral displacement at the top of the beam is:

$$v^{SV}(h) = \frac{Hh^3}{12EI} + \frac{Hh}{\kappa GA} + \frac{Hl^{SV}}{\kappa GA}\left\{\operatorname{csch}\left(\frac{h}{l^{SV}}\right)\left[\cosh\left(\frac{h}{l^{SV}}\right) - 1\right]^2 - \sinh\left(\frac{h}{l^{SV}}\right)\right\} \tag{62}$$

where $l^{SV} = \sqrt{EJ/\kappa GA}$ is the corresponding characteristic length.

The squatness of an element can be represented by $\Omega = EI/GAh^2$, which acquires large values as the length-to-depth ratio decreases. For an isotropic homogeneous beam with $E = 3G$ and a length-to-depth ratio of 0.5, $\Omega = 1$. As indicated before, however, for composite elements which are soft in shear Ω can acquire much larger values; for example, $10 \leq \Omega \leq 10,000$ for elastomeric bearings with moderate-to-high shape factor. Fig. 5 shows how the theories predict vastly different displacements in that range. The displacement predicted by the Shi-Voyiadjis beam unrealistically tends to vanish as Ω increases due to the constraint $\phi = \bar{\gamma}$, which forces the shear to vanish at the restrained ends. Simo's theory, despite also following this constraint, is not overly stiff because warping cannot be restrained due to the variational inconsistency. On the other hand, Kelly's formulation does account for the warping restraint at the ends, but the lateral displacement does not vanish even at high Ω values.

Critical load

The distinct nonlinear material assumptions in the theories lead to further differences in their critical load estimates. This is shown in Fig. 6, where Haringx's and Engesser's theories, which neglect cross-sectional distortions, have been included for reference. The buckling load from the proposed theory is significantly reduced with respect to Haringx's load, due to the cross-sectional distortion. Simo's critical load is significantly lower, and as $\Omega \to \infty$ it converges to $P_{cr}^S = \kappa GA/(1-\kappa)$ as a consequence of not accounting for the effect of warping restraint at the ends. On the other hand, Challamel's estimation is low at first and close to Engesser's solution for small values of Ω. However, as $\Omega \to \infty$ it converges to $P_{cr}^C = P_E EJ/(EI + EJ)$, exceeding even Haringx's load. This has not been duly noted in the derivation of this type of theories in (Wang et al. 2000; Challamel et al. 2013), where the analysis has been restricted to small values of Ω corresponding to more slender elements which are not affected as much by warping effects.

The theories exhibit significantly different behaviors for large values of Ω, which corresponds to the range of interest for short shear-flexible composite elements, including elastomeric bearings. In this range, constraining the warping amplitude $\phi = \bar{\gamma}$ leads to an overly stiff response. Theories that enforce this constraint, such as the one by Challamel, might still be useful for other applications using more slender elements corresponding to the context in which they were presented. However, the influence of warping decreases in such cases and the use of buckling theories that account for first-order shear might be accurate enough and lead to simpler solutions. Moreover, given that a variational approach at the stress-strain level is necessary to establish the linear equations corresponding to higher-order beam theories, it is deemed necessary to follow the same approach for the nonlinear equations. This would provide more insight about simplifications embedded in these so-called Engesser type theories, their applicability, and limitations. In Simo's formulation, however, the effects of the warping constraint are offset by its variational inconsistency.

APPLICATION TO FIBER-REINFORCED ELASTOMERIC ISOLATORS

The work presented heretofore, while being of particular interest for elements with large EA/GA and EI/GAh^2 ratios (e.g., elastomeric bearings), is general and applicable to any prismatic beam-like element. The subsequent discussion, however, is specific to FREIs, which have been proposed to seismically isolate normal-importance structures such as residential buildings. Stability under compressive loads is a critical aspect of their design (Pauletta 2019), and of elastomeric isolators in general (Constantinou et al. 2007). In the following, the proposed formulation is applied to evaluate the stability of unbonded infinite strip FREIs under no initial lateral displacement, and the results are compared to existing formulations. The results are validated with finite element analyses, providing a proof-of-concept on the applicability of the formulation. The case of FREIs with rectangular, circular and annular cross sections will be presented in a forthcoming publication. The results presented hereinafter also provide a foundation for the evaluation of the stability of FREIs under lateral displacement due to seismic loading, which often corresponds to the most critical design condition; such topic, however, is reserved for future studies.

Effective Isolator Properties

The mechanical response of an elastomeric isolator is governed by the composite action of the rubber and the reinforcement. The non-homogeneous material distribution along the isolator's axis leads to different axial stresses than those that occur in an element with constant material distribution along its axis. Hence, a homogenization of the isolator properties is needed to reconcile the beam theory with the isolator response. *Effective* rigidities and cross-sectional properties are obtained by evaluating the mechanical response of a single rubber layer of thickness t_e using the so-called pressure solution (Gent and Meinecke 1970; Kelly and Konstantinidis 2011). The kinematic assumptions are that vertical lines are deformed into a parabola, while the vertical displacement is assumed to vary linearly throughout the pad. Moreover, infinitesimal elasticity theory is employed for the rubber material as well as the reinforcement. It is further assumed that the normal stresses are dominated by the pressure p, such that $\sigma_{xx} \approx \sigma_{yy} \approx \sigma_{zz} \approx -p$.

The effective rigidities and cross-sectional properties for a planar infinite strip bearing with depth $2b$ are presented next. Let us define the following dimensionless parameters:

$$\alpha^2 = \frac{12Gb^2}{E_f t_f t_e} = \frac{12Gt_e S^2}{E_f t_f} \qquad \beta^2 = \frac{12Gb^2}{K t_e^2} = \frac{12GS^2}{K} \qquad \lambda^2 = \alpha^2 + \beta^2 \tag{63}$$

where K = bulk modulus of the rubber, E_f = Young's modulus of the fiber, t_f = thickness of the fiber, and S = shape factor, defined as the ratio of loaded area to area free to bulge in a single rubber layer. For an infinite strip layer, $S = b/t_e$. The parameter α measures fiber extensibility, while β measures the rubber compressibility; in practical scenarios, both terms are small but have important effects in the estimated rigidities, particularly when S is large.

The effective axial rigidity $\widetilde{EA}$ and effective bending rigidity $\widetilde{EI}$ accounting for bulk compressibility of the rubber and fiber extensibility are then given by (Kelly and Takhirov 2002):

$$\widetilde{EA} = \frac{24bGS^2}{\lambda^2}\left(1 - \frac{\tanh(\lambda)}{\lambda}\right) \tag{64}$$

$$\widetilde{EI} = \frac{24b^3GS^2}{\lambda^4}\left(1 + \frac{\lambda^2}{3} - \frac{\lambda}{\tanh(\lambda)}\right) \tag{65}$$

The derivation of the effective rigidity and cross-sectional properties associated with warping considering fiber extensibility but not rubber compressibility has been presented by Tsai and Kelly (2005a). To account for bulk compressibility of the rubber, the same procedure is followed with the sole modification that the trace of the infinitesimal strain tensor $\boldsymbol{\varepsilon}$ does not vanish and is given by $\mathrm{tr}(\boldsymbol{\varepsilon}) = -p/K$. Hence, only the relevant results are presented next.

First, the parameter ω in Eq. (7) is obtained from satisfying the third and fourth conditions in

Eq. (5). The third condition is trivially satisfied, and the fourth allows us to obtain:

$$\omega = -\left(\frac{1}{2} + \frac{3}{\lambda^2} + \frac{1}{5}\,\frac{\lambda^2}{3\lambda\coth(\lambda) - 3 - \lambda^2}\right) \tag{66}$$

Then, the warping rigidity and warping-related shear rigidities and cross-sectional areas are:

$$\widetilde{EJ} = -\frac{10b^3GS^2}{9\lambda^2}\left(\frac{3}{14} + \omega\right) \tag{67}$$

$$GB = \frac{5}{6}\,Gb\,(1 + 2\omega) \qquad GC = \frac{5}{72}\,Gb\left(9 + 20\omega + 20\omega^2\right) \tag{68}$$

$$\begin{gathered} f_B = \frac{5}{6}\,b\left(3 + 2\omega + \frac{6}{\lambda^2} - \frac{2\lambda}{\lambda - \tanh(\lambda)}\right) \\ f_C = \frac{5}{72}\,b\left(9 + 20\omega + 20\omega^2 + \frac{60\,(3 + 2\omega)}{\lambda^2} + \frac{1080}{\lambda^4} - \frac{360/\lambda^2 + 36 + 40\omega}{\lambda\coth(\lambda) - 1}\right) \end{gathered} \tag{69}$$

When steel reinforcement is present, further modifications need to be implemented to account for its bending rigidity (Tsai and Kelly 2005a). When fiber is used, it is reasonable to assume the reinforcement as completely flexible in bending, forgoing the need for these modifications.

Finite Element Analysis

To evaluate the suitability of the different theories in the prediction of the buckling load of FREIs, a finite element study was developed using the nonlinear FEA software `Marc` (MSC Software 2021). A parametric study was carried out for two-dimensional plane strain models representing the infinite strip bearings described above. The bearings are modeled in an unbonded configuration where they remain in place due to the pressure and friction between the bearings and their supports. The analysis and its results are presented in the following.

Modeling

The finite element analysis was carried out using mixed-formulation low-order elements, which prevent volumetric locking while being robust with respect to mesh distortions. The formulation employed extends from a Hu-Washizu type three-field variational principle proposed by Simo et al. (1985) defined in terms of the deformation $\boldsymbol{\varphi}$, the pressure p, and the volumetric strain θ. The corresponding functional is given by:

$$\Pi(\boldsymbol{\varphi}, p, \theta) = \int_{\mathcal{B}} \left[\hat{W}(\hat{\mathbf{C}}) + U(\theta) + p\,(J - \theta) \right] dV + \Pi_{ext}(\boldsymbol{\varphi}) \tag{70}$$

where $\Pi_{ext}(\boldsymbol{\varphi})$ = the external potential energy due to the imposed body forces and surface tractions. The functional $\Pi(\boldsymbol{\varphi}, p, \theta)$ adopts the following multiplicative split of the deformation gradient:

$$\bar{\mathbf{F}} = \theta^{1/3}\,\hat{\mathbf{F}}, \tag{71}$$

where $\hat{\mathbf{F}} = J^{-1/3}\,\partial\boldsymbol{\varphi}/\partial\mathbf{X}$ corresponds to the isochoric part of the deformation gradient, leading to the modified right Cauchy-Green deformation tensor $\hat{\mathbf{C}} = \hat{\mathbf{F}}^{\top}\hat{\mathbf{F}}$. An additive split of the strain energy $W(\bar{\mathbf{C}}) = \hat{W}(\hat{\mathbf{C}}) + U(\theta)$ has been assumed, where $\hat{W}$ and U are the deviatoric and volumetric parts of the strain energy, respectively.

Many phenomenological and statistical mechanics constitutive models for elastomeric materials are available. However, most of these models depend on a large number of parameters, which makes them unsuitable for a parametric study such as the one pursued here. Hence, a simple compressible neo-Hookean model defined by the shear modulus G and bulk modulus K was used for the rubber. The deviatoric strain energy is then given by:

$$\hat{W}(\hat{\mathbf{C}}) = \frac{G}{2}\,(I_{\hat{\mathbf{C}}} - 3) \tag{72}$$

where $I_{\hat{\mathbf{C}}}$ = the first invariant of $\hat{\mathbf{C}}$. The selected volumetric strain energy function is:

$$U(\theta) = K\left(\frac{\theta^2 - 1}{4} - \frac{\ln\theta}{2}\right) \tag{73}$$

A fine mesh was required to achieve convergence of the buckling loads and capture the high distortion of the bulging ends of the bearing (see Fig. 7). Triangular elements were used at the edges of the bearings to avoid the failure of the quadrilateral elements due to excessive distortion, while quadrilateral elements were used at the inner part of the bearings. Moreover, an unstructured mesh was used for the sections with triangular elements to smoothly transition between a coarser mesh at the inner section and a finer mesh at the edges. The algorithm presented by Persson and Strang (2004) was implemented for this purpose.

The quadrilateral elements correspond to Q1-P0 elements, which use continuous piecewise bilinear interpolation for the deformation field and piecewise constant interpolation for the pressure and volumetric strain fields (Simo et al. 1985). In `Marc` this corresponds to element type 11 with constant dilation. The triangular elements correspond to a variation of the so-called MINI element (Arnold et al. 1984), which makes use of continuous linear interpolation for the deformation field augmented by a bubble function, continuous piecewise linear interpolation for the pressure and discontinuous constant interpolation for the volumetric strain. In `Marc` this corresponds to element 155. Both elements are implemented in an Updated Lagrangian formulation.

The reinforcement was modeled using tension-only two-node plane strain rebar elements, corresponding to `Marc` element type 165. These elements only have a displacement field for which they use linear interpolation, and thus they do not have any flexural rigidity. They are implemented in a Total Lagrangian formulation. The material for the fiber reinforcement is linear elastic, defined by its Young's modulus E_f and Poisson's ratio ν_f. Moreover, a node-to-segment formulation was implemented to handle the contact between the bearing and its supports, and the bearing with itself. The top and bottom supports were represented as rigid curves, while Coulomb friction was implemented using a bilinear formulation. Preliminary analyses evidenced negligible influence of the friction coefficient μ on the results. Therefore, μ was fixed at 1.0 for all the simulations.

Buckling Analysis Method

The buckling load was determined by performing linearized buckling analyses with respect to an equilibrium configuration of the bearing, which is obtained from a fully nonlinear analysis (see Riks 1997). This is implemented using the `buckle` routine in `Marc` (MSC Software 2021). A vertical load $P = \xi P_{ref}$ is applied to the model, with P_{ref} a reference vertical load and ξ the load factor that defines the magnitude of the applied load. Then, for a given equilibrium configuration i with load factor ξ_i, the following eigenvalue problem is solved:

$$\left[\mathbf{K}(\xi_i) + (\xi^* - \xi_i)\left.\frac{d\mathbf{K}(\xi)}{d\xi}\right|_{\xi=\xi_i}\right]\mathbf{u}^* = \mathbf{0} \tag{74}$$

where $\mathbf{K}(\xi_i)$ = the stiffness matrix, and $[d\mathbf{K}(\xi)/d\xi]_{\xi=\xi_i}$ = change in the stiffness matrix with respect to the load factor ξ, both evaluated at the equilibrium configuration i.

The solution of the eigenvalue problem gives an estimate of the buckling load $P^* = \xi^* P_{ref}$ and the buckling mode shape $\mathbf{u}^*$. When the approximate critical equilibrium state is close enough to the equilibrium configuration from which it was calculated, the influence of the initial deformation of the body is properly accounted for in the calculation; in this study the eigenvalue solution has been accepted when $(\xi^* - \xi_i)/\xi_i < 0.02$. Moreover, when the equilibrium configuration i is far from the critical equilibrium configuration, the eigenvalue problem might yield spurious solutions which correspond to nonphysical instabilities of the model. Thus, the eigenmode $\mathbf{u}^*$ needs to be checked to guarantee that it corresponds to a physical lateral buckling mode. When both of the previous conditions are met, $\xi_{cr} \approx \xi^*$ such that $P_{cr} = \xi_{cr} P_{ref}$ and $\mathbf{u}_{cr} = \mathbf{u}^*$ (see Fig. 8).

Cases

The influence of various parameters on the buckling load was evaluated. The geometric parameters considered include the shape factor $S = b/t_e$, which affects all of the effective rigidities [Eqs. (64), (65) and (67)], and the width-to-total height aspect ratio $S_2^* = 2b/h$ [cf. the second shape factor $S_2 = 2b/t_r$, where t_r = total thickness of elastomer] which measures the overall slenderness of the isolator; b, h and t_e are as previously defined. The material parameters evaluated were the shear modulus G, the bulk modulus K, and the reinforcement Young's modulus E_f. The values for these parameters included in the analysis are presented in Table 1, and provide realistic ranges for unbonded FREIs used in seismic isolation. Each parameter was varied while the rest were set to their default values. The total height of the bearings was fixed at $h = 100$ mm, while the fiber thickness was $t_f = 0.50$ mm. Note that the exact S values used differed slightly from the target values listed in Table 1 because the bearing geometry was constrained to satisfy the S_2^* values exactly. In total, 260 cases were analyzed; geometric parameter combinations that yielded fewer than 5 or more than 20 rubber layers were not included because they do not correspond to realistic bearing designs.

Results

The first theoretical formulation compared with the FEA results is the complete higher-order expression [Eq. (45)], hereinafter referred to as the *proposed-exact* equation. The simplified expression shown in Eq. (47), hereinafter referred to as the *proposed-approximate* equation, is also compared. In both of these formulations, the effective cross-sectional properties account for compressibility of the rubber and extensibility of the reinforcement. Moreover, results based on Simo's and Haringx's theories are included for comparison purposes. Both of them have been implemented as originally introduced and, in the case of Haringx, currently used in practice: disregarding the influence of rubber compressibility and reinforcement extensibility on the cross-sectional effective properties. From a theoretical standpoint, Haringx's theory provides an upper bound for the buckling load estimation of an isolator that is flexible in warping.

Fig. 9 shows that the FEA results are approximately bounded from below by the proposed-exact formulation, and from above by Haringx's theory; in this figure, each combination of line (and marker) color and style is associated with a unique combination of width-to-height aspect ratio and analytical (or numerical) formulation. The proposed-exact expression closely agrees with the numerical results, except for combinations of low shape factors and high aspect ratios where it underestimates them. The proposed-approximate equation is in excellent agreement with the exact one, exhibiting the same trends and approaching it closely from below. In contrast, Simo's theory significantly underestimates the load of critical equilibrium which extends from neglecting the effect of the warping restraint at the element ends. Due to the squat geometry of the bearings, this has a significant influence in their nonlinear behavior, which Simo's theory does not capture. Despite increasing with an increasing shape factor, the FEA estimates of the critical load present a lower sensitivity with respect to S than expected from the proposed formulation. This agrees with the findings presented by Galano et al. (2021).

Using the FEA results as benchmark, Fig. 10 compares the performance of the analytical formulations with respect to the average compressive strain at buckling $\varepsilon_{c,cr} = \Delta_{cr}/h$, where Δ_{cr} = the vertical displacement at buckling. The performance of the proposed formulations decreases with increasing $\varepsilon_{c,cr}$, even for the proposed-exact solution that accounts for the axial shortening. As opposed to steel-reinforced elastomeric isolators, FREIs typically have smaller shape factors and more axially flexible reinforcement, leading to large shortening at buckling for some of the analyzed bearings. Due to the quasi-incompressibility of the rubber, this causes a nonlinear increase of the cross section that is not negligible, which increases the bending and warping rigidity of the bearing. Such behavior cannot be accounted for in one-dimensional theories as the ones dealt with herein where the cross-sectional dimensions remain constant. Proper consideration of these effects would require the analysis of the three-dimensional problem.

Similar behavior has been reported in the context of low-shape factor ($S < 5$) steel-reinforced elastomeric bearings for bridges or 3D seismic isolation (Stanton et al. 1990; Orfeo et al. 2023). In those cases, the significant cross-sectional expansion under compression of the axially flexible steel-reinforced elastomeric bearings has been deemed to have a major influence on the stability of the bearings. Semi-empirical correction factors have been proposed in those instances to account for cross-sectional expansion and improve the accuracy of the P_{cr} estimates. Such an approach is not pursued here considering that bearings exhibiting large compressive strains would not be implemented for standard seismic isolation purposes—the focus of this work. Moreover, the influence of these effects is accentuated in the present results due to the plane strain conditions, but it becomes less relevant for the three-dimensional cases.

The influence of the different material properties is illustrated in Fig. 11 where, again, each combination of line (and marker) color and style corresponds to a unique combination of width-to-height aspect ratio and analytical (or numerical) method. The variation of the critical loads with respect to the rubber's shear modulus G is similar in all the analytical formulations and the FEA results, as shown in Fig. 11; note that P_{cr} has been normalized by G in Fig. 11(a), and thus a horizontal line represents a linear relation between them. A linear increase of the critical load with respect to the rubber's shear modulus is expected for Haringx's theory. Simo's theory, which converges to $P_{cr}/A = 5G$, naturally exhibits a linear relation, too. The same would apply for the proposed formulations, were it not for the inclusion of the rubber compressibility in the effective rigidities which leads to a slightly nonlinear increase of the buckling load with respect to G. The numerical results also exhibit a slightly nonlinear increase with respect to the rubber's shear modulus.

Haringx's and Simo's theories were implemented without accounting for rubber compressibility and fiber extensibility in the estimation of the bearing effective properties. Therefore, neither formulation is affected by these properties in Fig. 11(b). The proposed formulations do account for these effects through parameter λ [Eq. (63)], which tends to reduce the effective rigidities as the rubber becomes more compressible and the reinforcement more axially flexible, hence reducing P_{cr}. These effects are more important for large shape factors, as λ is proportional to S, and thus only the results for $S = 30$ are presented in Fig. 11. As seen in Fig. 11(b,c), the behavior of the FEA results with respect to the normalized bulk modulus and the normalized reinforcement axial rigidity is in agreement with that of the proposed formulations.

The effect of rubber compressibility becomes noticeable for K/G ratios lower than 5000, while it does not affect P_{cr} significantly outside that range. In contrast, within the range of the evaluated material parameters, the critical loads (both analytical and numerical) are quite insensitive to the reinforcement extensibility, even for a high shape factor of $S = 30$ [see Fig. 11(c)]. The material parameters adopted in the numerical study cover the range of expected reinforcement axial rigidity. Thus, the results indicate that for realistic scenarios, the reinforcement extensibility has a negligible effect on the isolator's critical load. This result is relevant because neglecting the fiber's extensibility allows to simplify the computation of the isolator's effective rigidities.

Towards Practical Implementation

Both proposed formulations exhibit excellent agreement, but the approximate one is deemed more convenient for practical implementation because it is given in closed-form and requires fewer additional warping properties. Its performance with respect to the numerical results is compared to Haringx's theory in Fig. 12. The effective rigidities required for each theory have been calculated under four scenarios: (1) considering both rubber compressibility and fiber extensibility, (2) considering only rubber compressibility ($\alpha = 0$), (3) considering only fiber extensibility ($\beta = 0$), and (4) considering neither rubber compressibility nor fiber extensibility ($\alpha = \beta = 0$). Results presented in the figure correspond to average ratios of the analytical to numerical buckling loads over all the combinations of material parameters. Nevertheless, the results for any specific triad of G, K and E_f follow the same trends as can be interpreted from the low coefficients of variation, shown in Fig. 13. Simo's theory has been excluded from the comparison because it substantially underestimates P_{cr} for all the studied cases.

Practically feasible geometric parameter ranges for FREIs, which correspond to aspect ratios between 2.0 - 5.0 and shape factors larger than 10, are highlighted with dashed-line rectangles in Figs. 12 and 13. An aspect ratio of 2.0 - 2.5 has been shown experimentally (Toopchi-Nezhad et al. 2008) and analytically (Van Engelen et al. 2015) to be the threshold at which instability under lateral deformation due to rollover effects is precluded in unbonded FREIs. Isolators with lower aspect ratios will become unstable under lateral deformation before the originally vertical faces of the bearing contact the supports, making them unsuitable for seismic isolation applications. On the other hand, $S = 10$ corresponds to a practical lower limit to prevent the bearing from being overly flexible in compression and avoid coupling of lateral and vertical structural vibration modes.

Haringx's theory can become largely unconservative for geometric parameter combinations that yield feasible designs for isolation purposes (ratios larger than one in Fig. 12). The proposed-approximate expression underpredicts the buckling loads for low shape factors but tends to be close to the numerical results (unity in Fig. 12) in the highlighted region of interest. When fiber extensibility is neglected ($\alpha = 0$), the mean ratios are slightly modified (Fig. 12), but the variation of the ratios for specific material combinations (G, K, E_f) with respect to the mean ratios (Fig. 13) is actually reduced. This coincides with the negligible influence of the reinforcement axial rigidity on the critical load previously identified. Based on this, the use of the proposed-approximate expression in Eq. (47) along with effective bearing properties that account for rubber compressibility can provide a good estimation of the buckling load of unbonded FREIs.

CONCLUSIONS

A buckling theory for short beams that accounts for shear warping was developed based on the consistent linearization of the geometrically nonlinear planar problem. The assumed deformation field considers the warping amplitude as an independent generalized displacement, which proves to be a critical point for the adequacy of the theory. An appropriate hyperelastic material was proposed in terms of the stresses normal and tangent to the deformed cross section by assuming linearity of these stresses with respect to their work-conjugate strains, established based on stress power considerations. The solution for the critical load of a beam with fixed supports but free-to-sway at the top yields a quartic equation which can be solved by iteration. If the axial shortening of the element is neglected, this formulation coincides with the Kelly-Tsai theory. An approximate closed-form solution is provided for the critical load which allows a clear understanding of the reduction due to the warping effects with respect to the classical theory of Haringx.

The proposed formulation is compared to Simo's theory, developed for elastomeric bearings, and Challamel's buckling solution for the Shi-Voyiadjis beam, which is representative of the so-called Engesser-approach often used for the buckling of higher-order shear beams. It was shown that constraining the warping amplitude to be proportional to the average shear leads to an overly stiff response, with unrealistically vanishing shear deformations for short elements. Variational consistency is a strict requirement and failure to satisfy it, as in Simo's approach, yields to omission of higher-order resultants and overly flexible formulations tantamount to solutions with unrestrained warping. Lastly, it is demonstrated that the material assumptions embedded in Simo's and Kelly-Tsai theories are simplified second-order approximations of the material constitutive relation proposed herein. It is further shown that Engesser-approaches cannot be directly traced back to a specific material constitutive relation, and simplifying assumptions that justify Engesser's solution for first-order shear beams are not applicable for higher-order shear elements.

The proposed analytical formulation closely matched the numerical results from the finite element parametric study for unbonded infinite strip FREIs with moderate-to-high shape factors corresponding to realistic designs for seismic isolation purposes. It only underestimated the critical loads for bearings with low shape factor and high width-to-height aspect ratio, which exhibit significant axial shortening at buckling, leading to a nonlinear increase in cross-sectional dimensions not accounted for in one-dimensional theories. The inclusion of compressibility effects in the effective rigidities was shown to be important for bearings with high shape factors, but axial extensibility of the reinforcement showed negligible influence in the results and can be neglected. The approximate closed-form solution for the proposed theory exhibits excellent agreement with the proposed-exact solution and numerical results, and is deemed suitable for practical implementation. Instead, Haringx's theory was shown to largely overestimate the buckling capacity of FREIs, and its use for this application is discouraged. Experimental validation of the proposed theory is recommended for future studies to supplement the numerical validation presented herein.

DATA AVAILABILITY STATEMENT

All data, models, and code generated that support the findings of this study are available from the corresponding author upon reasonable request.

ACKNOWLEDGEMENTS

Comments by Professor Francisco Armero on a draft of the manuscript are appreciated.

References

Armero, F. (2022). "On the modeling of restrained torsional warping: an analysis of two formulations." *Zeitschrift für angewandte Mathematik und Physik*, 73(2), 56.

Arnold, D. N., Brezzi, F., and Fortin, M. (1984). "A stable finite element for the stokes equations." *CALCOLO*, 21(4), 337–344.

Barber, J. R. (2010). *Elasticity*. Springer, Dordrecht, 3 edition.

Bažant, Z. P. and Cedolin, L. (2010). *Stability of Structures*. World Scientific, Singapore.

Bickford, W. B. (1982). "A consistent higher order beam theory." *Developments in Theoretical and Applied Mechanics*, 11, 137–150.

Challamel, N. (2011). "Higher-order shear beam theories and enriched continuum." *Mechanics Research Communications*, 38(5), 388–392.

Challamel, N., Mechab, I., El Meiche, N., Houari, M. S. A., Ameur, M., and Atmane, H. A. (2013). "Buckling of generic higher-order shear beam/columns with elastic connections: Local and nonlocal formulation." *Journal of Engineering Mechanics*, 139(8), 1091–1109.

Constantinou, M. C., Whittaker, A. S., Kalpakidis, Y., Fenz, D. M., and Warn, G. P. (2007). "Performance of seismic isolation hardware under service and seismic loading." *Report No. MCEER-07-0012*, Multidisciplinary Center for Earthquake Engineering Research, Buffalo, New York.

El Meiche, N., Tounsi, A., Ziane, N., Mechab, I., and Adda.Bedia, E. A. (2011). "A new hyperbolic shear deformation theory for buckling and vibration of functionally graded sandwich plate." *International Journal of Mechanical Sciences*, 53(4), 237–247.

Engesser, F. (1891). "Die knickfestigkeit gerader stäbe." *Centralblatt der Bauverwaltung*, 11(49), 483–486.

Galano, S., Losanno, D., and Calabrese, A. (2021). "Stability analysis of unbonded fiber reinforced isolators of square shape." *Engineering Structures*, 245, 112846.

Gent, A. N. (1964). "Elastic stability of rubber compression springs." *Journal of Mechanical Engineering Science*, 6(4), 318–326.

Gent, A. N. and Meinecke, E. A. (1970). "Compression, bending, and shear of bonded rubber blocks." *Polymer Engineering & Science*, 10(1), 48–53.

Habieb, A. B., Valente, M., and Milani, G. (2019). "Implementation of a simple novel Abaqus user element to predict the behavior of unbonded fiber reinforced elastomeric isolators in macro-scale computations." *Bulletin of Earthquake Engineering*, 17, 2741–2766.

Haringx, J. A. (1949). "On highly compressible helical springs and rubber rods, and their application for vibration-free mountings, III." *Report No. Philips Res. Rep. 4*, Philips Research Laboratories, Eindhoven, Netherlands.

Holzapfel, G. A. (2000). *Nonlinear Solid Mechanics: A Continuum Approach for Engineering*. John Wiley & Sons Ltd, Chichester.

Karama, M., Afaq, K. S., and Mistou, S. (2003). "Mechanical behaviour of laminated composite beam by the new multi-layered laminated composite structures model with transverse shear stress continuity." *International Journal of Solids and Structures*, 40(6), 1525–1546.

Kelly, J. M. (1994). "The influence of plate flexibility on the buckling load of elastomeric isolators." *Report No. UCB/EERC-94/03*, Earthquake Engineering Research Center, Berkeley, California.

Kelly, J. M. and Konstantinidis, D. (2011). *Mechanics of Rubber Bearings for Seismic and Vibration Isolation*. John Wiley & Sons Ltd.

Kelly, J. M. and Marsico, M. R. (2010). "Stability and post-buckling behavior in nonbolted elastomeric isolators." *Seismic Isolation and Protection Systems*, 1(1), 41–54.

Kelly, J. M. and Takhirov, S. M. (2002). "Analytical and experimental study of fiber-reinforced strip isolators." *Report No. PEER 2002/11*, Pacific Earthquake Engineering Research Center, Berkeley, California.

Konstantinidis, D., Kelly, J. M., and Makris, N. (2008). "Experimental investigations on the seismic response of bridge bearings." *Report No. EERC 2008-02*, Earthquake Engineering Research Center, Berkeley, California.

Love, A. E. H. (1944). *A Treatise on the Mathematical Theory of Elasticity*. Dover Publications, New York, 4 edition.

Moghadam, S. R. and Konstantinidis, D. (2017). "Finite element study of the effect of support rotation on the horizontal behavior of elastomeric bearings." *Composite Structures*, 163, 474–490.

Moghadam, S. R. and Konstantinidis, D. (2021). "Experimental and analytical studies on the horizontal behavior of elastomeric bearings under support rotation." *Journal of Structural Engineering*, 147(4), 04021024.

MSC Software (2021). *Marc 2021.4 Volume A: Theory and User Information*.

Orfeo, A., Tubaldi, E., and Muhr, A. H. (2023). "Mechanical behaviour of rubber blocks." *International Journal of Solids and Structures*, 271-272, 112259.

Pauletta, M. (2019). "Method to design fiber-reinforced elastomeric isolators (U-FREIs) and application." *Engineering Structures*, 197, 109366.

Persson, P.-O. and Strang, G. (2004). "A simple mesh generator in MATLAB." *SIAM Review*, 46(2), 329–345.

Reddy, J. N. (1984). "A simple higher-order theory for laminated composite plates." *Journal of Applied Mechanics*, 51(4), 745–752.

Reissner, E. (1972). "On one-dimensional finite-strain beam theory: The plane problem." *Zeitschrift für angewandte Mathematik und Physik ZAMP*, 23(5), 795–804.

Riks, E. (1997). "Buckling analysis of elastic structures: A computational approach." *Advances in Applied Mechanics*, E. van der Giessen and T. Y. Wu, eds., Vol. 34, Elsevier, 1–76.

Shi, G. and Voyiadjis, G. Z. (2010). "A sixth-order theory of shear deformable beams with variational consistent boundary conditions." *Journal of Applied Mechanics*, 78(2).

Simo, J. C. (1982). "A consistent formulation of nonlinear theories of elastic beams and plates." *Report No. UCB/SESM-82/06*, University of California, Berkeley, Berkeley, California.

Simo, J. C., Taylor, R. L., and Pister, K. S. (1985). "Variational and projection methods for the volume constraint in finite deformation elasto-plasticity." *Computer Methods in Applied Mechanics and Engineering*, 51(1), 177–208.

Simo, J. C. and Vu-Quoc, L. (1991). "A geometrically-exact rod model incorporating shear and torsion-warping deformation." *International Journal of Solids and Structures*, 27(3), 371–393.

Stanton, J. F., Roeder, C. W., Mackenzie-Helnwein, P., White, C., Kuester, C., and Craig, B. (2008). "Rotation limits for elastomeric bearings." *Report No. NCHRP Report 596*, National Cooperative Highway Research Program, Washington, D.C.

Stanton, J. F., Scroggins, G., Taylor, A. W., and Roeder, C. W. (1990). "Stability of laminated elastomeric bearings." *Journal of Engineering Mechanics*, 116(6), 1351–1371.

Strauss, A., Apostolidi, E., Zimmermann, T., Gerhaher, U., and Dritsos, S. (2014). "Experimental investigations of fiber and steel reinforced elastomeric bearings: Shear modulus and damping coefficient." *Engineering Structures*, 75, 402–413.

Timoshenko, S. and Goodier, J. N. (1970). *Theory of Elasticity*. McGraw Hill, New York, 3 edition.

Toopchi-Nezhad, H., Tait, M. J., and Drysdale, R. G. (2008). "Testing and modeling of square carbon fiber-reinforced elastomeric seismic isolators." *Structural Control and Health Monitoring*, 15(6), 876–900.

Touratier, M. (1991). "An efficient standard plate theory." *International Journal of Engineering Science*, 29(8), 901–916.

Tsai, H.-C. and Kelly, J. M. (2005a). "Buckling load of seismic isolators affected by flexibility of reinforcement." *International Journal of Solids and Structures*, 42(1), 255–269.

Tsai, H.-C. and Kelly, J. M. (2005b). "Buckling of short beams with warping effect included." *International Journal of Solids and Structures*, 42(1), 239–253.

Van Engelen, N. C. (2019a). "Fiber-reinforced elastomeric isolators: A review." *Soil Dynamics and Earthquake Engineering*, 125, 105621.

Van Engelen, N. C. (2019b). "Rotation in rectangular and circular reinforced elastomeric bearings resulting in lift-off." *International Journal of Solids and Structures*, 168, 172–182.

Van Engelen, N. C., Tait, M. J., and Konstantinidis, D. (2015). "Model of the shear behavior of unbonded fiber-reinforced elastomeric isolators." *Journal of Structural Engineering*, 141(7), 04014169.

Wang, C. M., Reddy, J. N., and Lee, K. H. (2000). *Shear Deformable Beams and Plates: Relationships with Classical Solutions*. Elsevier Science Ltd, Oxford, 1 edition.

List of Tables

Table 1. Parameters used for buckling analysis

Parameter	Value[a]
S	**5, 10, 15, 20, 25, 30**
S_2^*	**1, 2, 3, 4, 5**
G (MPa)	**0.4**, 0.6, 0.8, 1.0, 1.2
K (MPa)	**2000**, 4000, 6000, 8000, 10000
E_f (MPa)	**25000**, 50000, 75000, 100000, 125000

[a] Default cases shown in bold font.

List of Figures

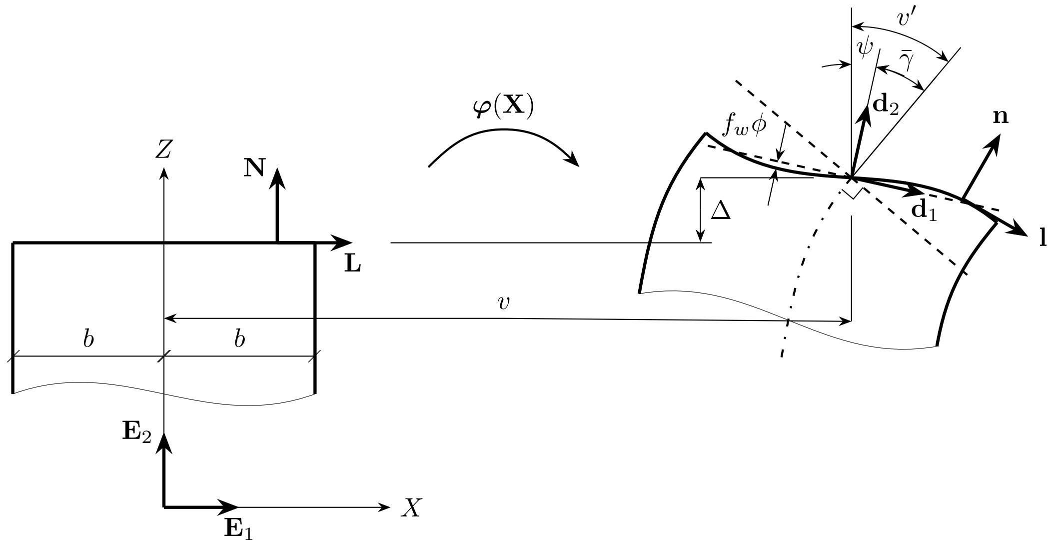

Figure 1. Generalized displacements and orthonormal frames

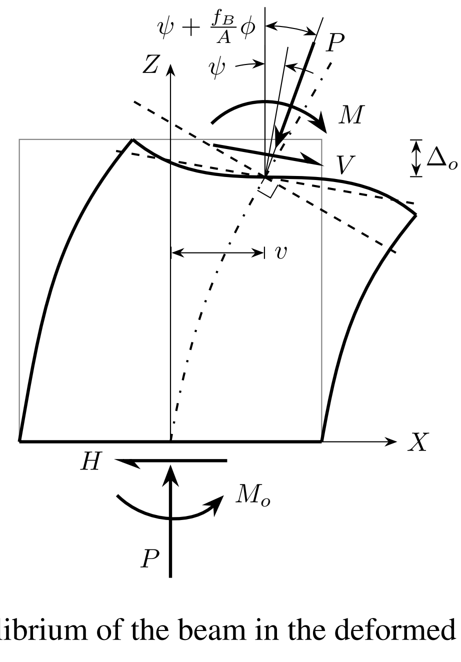

Figure 2. Equilibrium of the beam in the deformed configuration

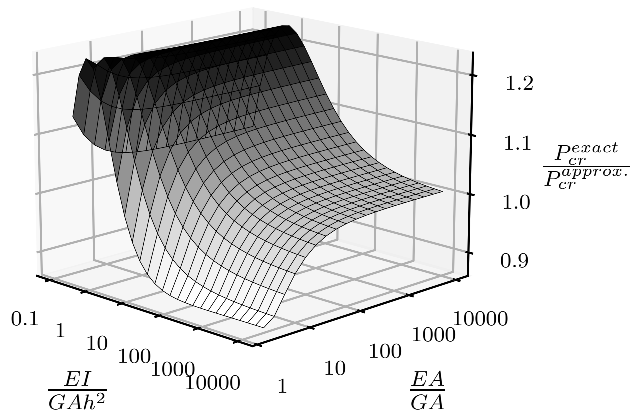

Figure 3. Ratio of proposed-exact P_{cr} [Eq. (45)] to proposed-approximate P_{cr} [Eq. (47)]

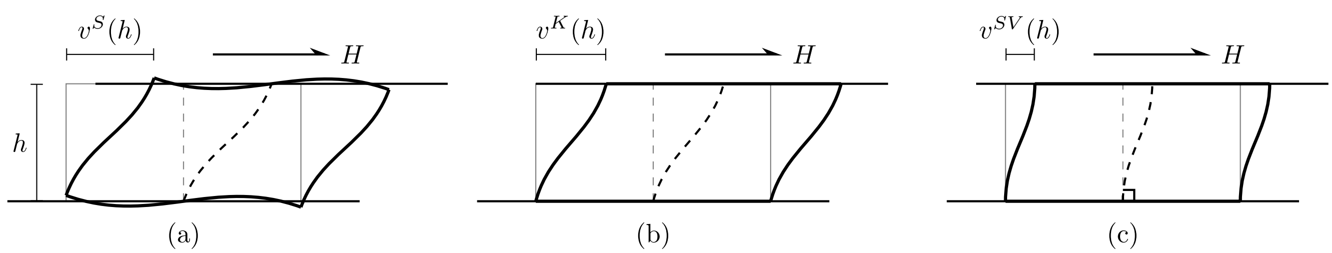

Figure 4. Lateral deformation using (a) Simo's beam, (b) Kelly's beam and (c) Shi-Voyiadjis beam

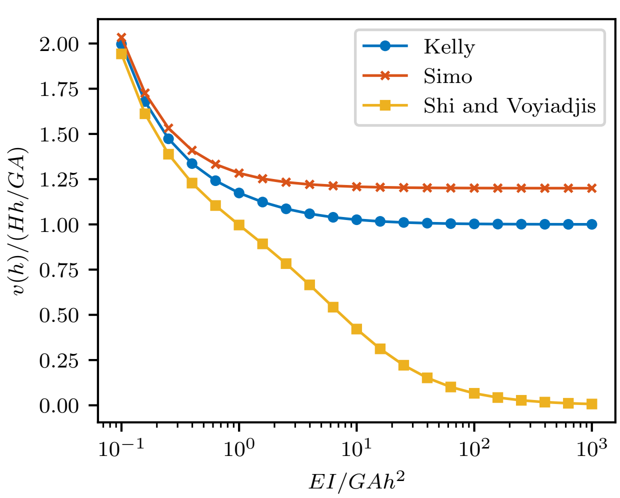

Figure 5. Influence of bending-to-shear stiffness ratio on the beam's top lateral displacement

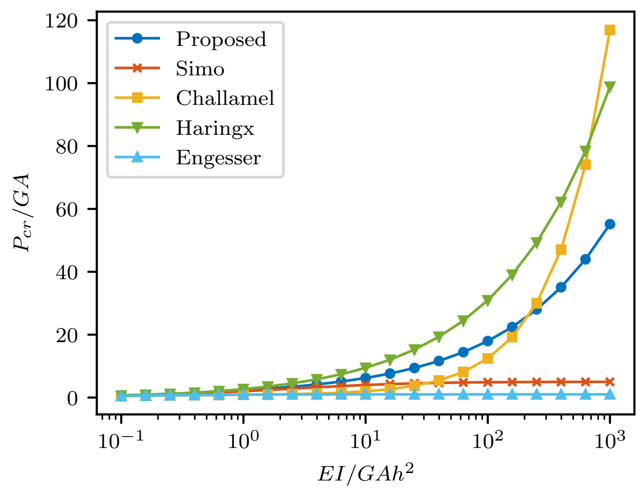

Figure 6. Influence of the bending-to-shear stiffness ratio on the buckling load

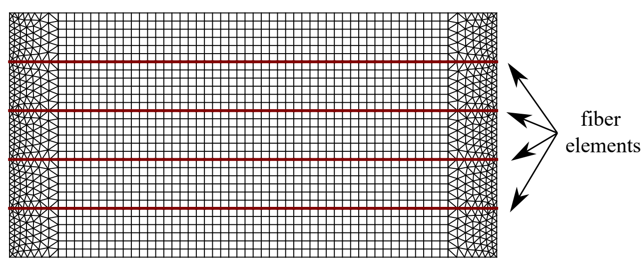

Figure 7. Mesh for a 200 mm × 100 mm isolator with shape factor $S = 5$

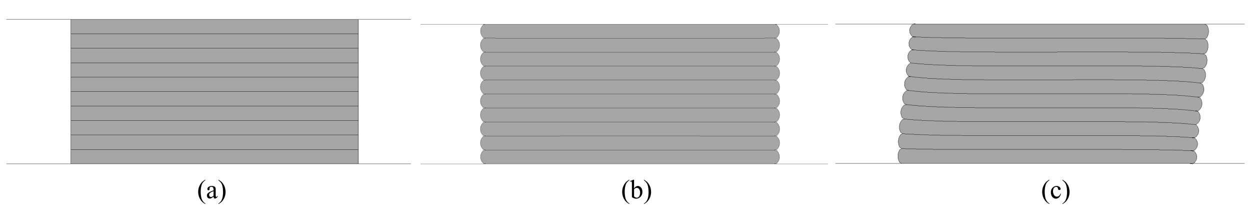

Figure 8. Loading sequence for a 200 mm × 100 mm isolator with shape factor $S = 10$: (a) undeformed isolator, (b) compressed isolator, (c) buckling mode shape

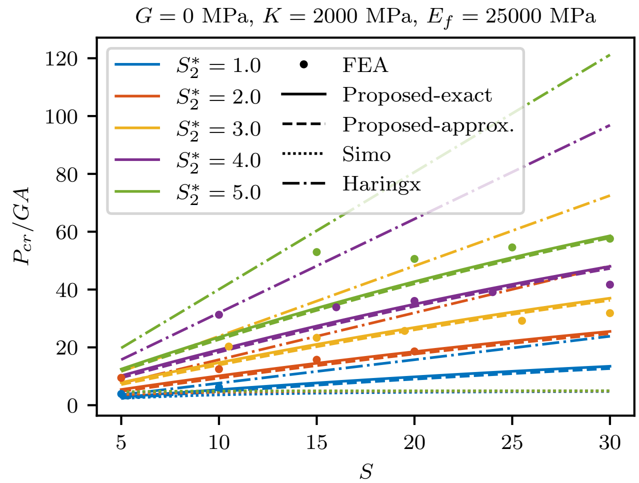

Figure 9. Comparison of different analytical and FEA solutions for the normalized buckling load as a function of shape factor

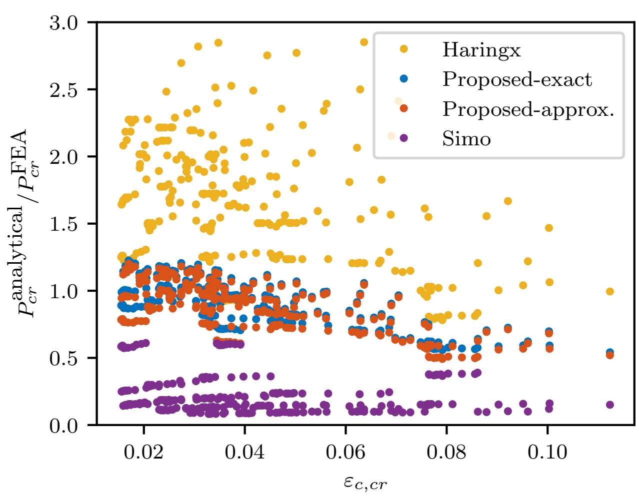

Figure 10. Analytical to FEA buckling load ratio with respect to average compressive strain at buckling

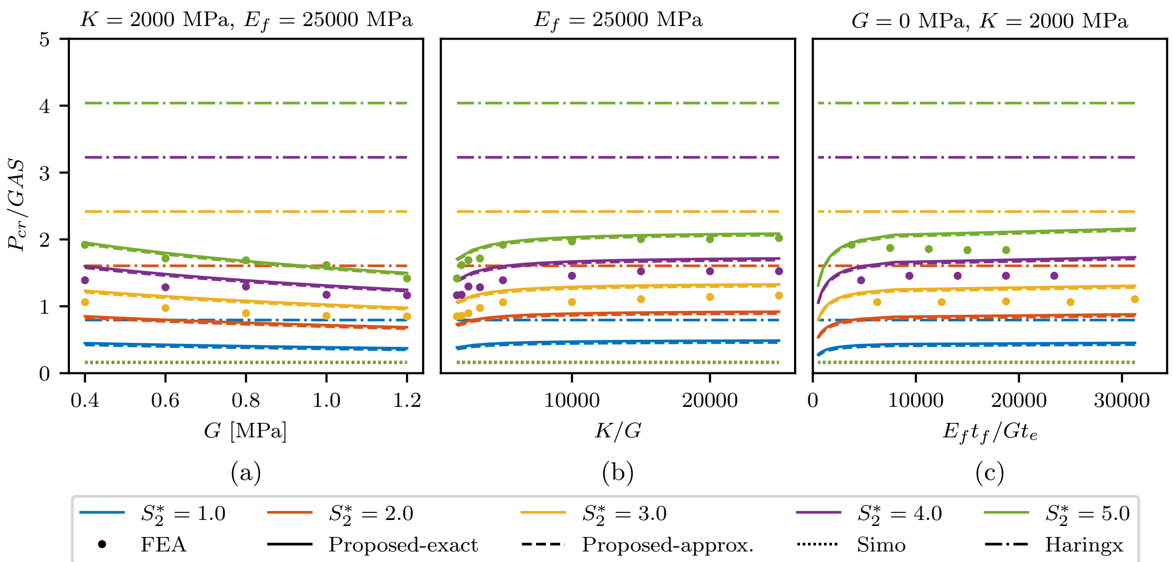

Figure 11. Normalized buckling load for isolators with shape factor $S = 30$ as a function of: (a) shear modulus, (b) compressibility, and (c) reinforcement extensibility

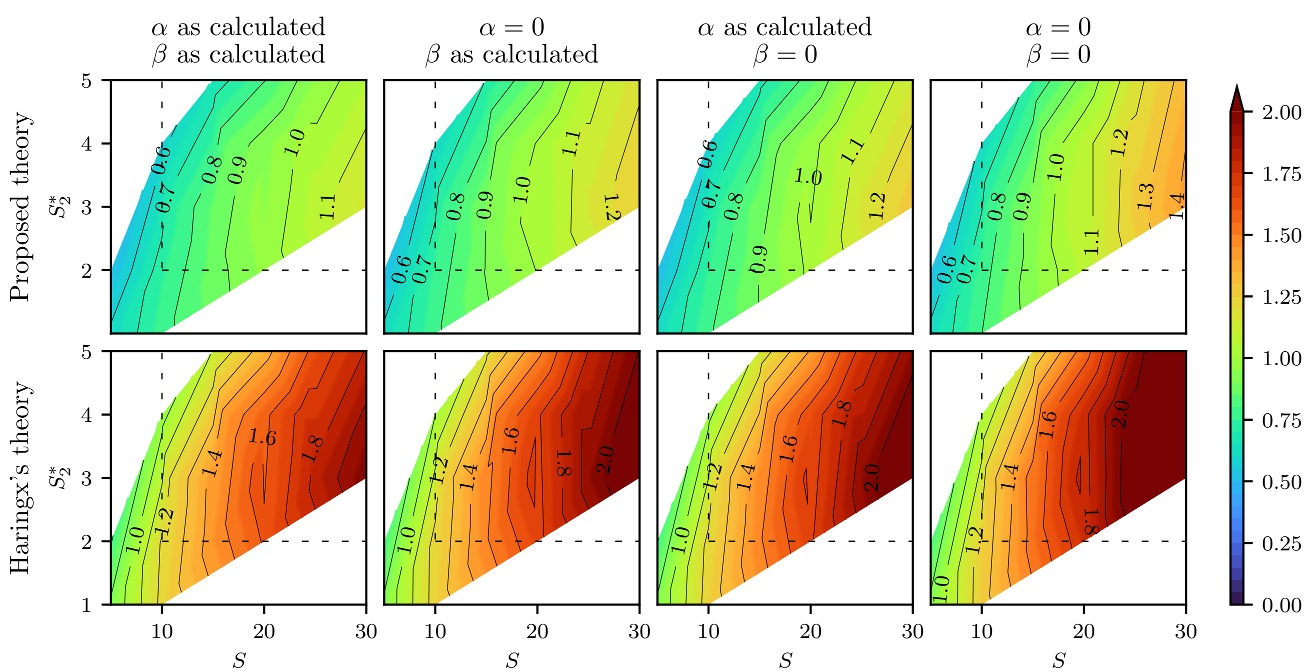

Figure 12. Average ratio $P_{cr}^{\text{analytical}}/P_{cr}^{\text{FEA}}$ depending on analytical formulation and method to calculate the effective rigidities

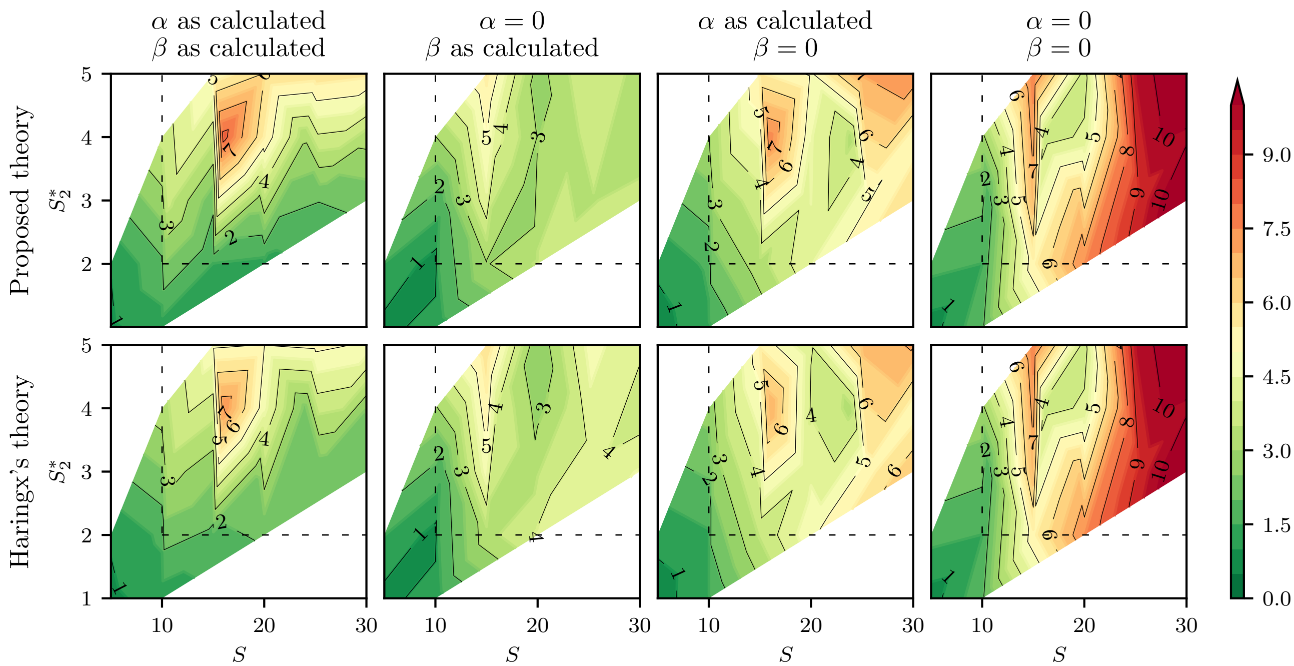

Figure 13. Coefficient of variation (%) of the ratio $P_{cr}^{\text{analytical}}/P_{cr}^{\text{FEA}}$ depending on analytical formulation and method to calculate the effective rigidities